DESIGN, ANALYSIS AND IMPLEMENTATION OF NARROW BEAM DIRECTIVE SMALL SIZE ANTENNAS IN 0.5–3 GHz BAND

by

Ashrf AOAD

May 2011

DESIGN, ANALYSIS AND IMPLEMENTATION OF NARROW BEAM DIRECTIVE SMALL SIZE ANTENNAS IN 0.5–3 GHz BAND

by

Ashrf AOAD

A thesis submitted to

The Graduate Institute of Sciences and Engineering

of

Fatih University

in partial fulfillment of the requirements for the degree of

Master of Science

in

Electrical and Electronics Engineering

May 2011

Istanbul, Turkey

APPROVAL PAGE

I certify that this thesis satisfies all requirements as a thesis for the degree of Master of Science.

Assoc. Prof. Onur TOKER
Head of department

This is to certify that I have read this thesis and that in my opinion it is fully adequate, in scope and quality for the degree of Master of Science.

Assist. Prof. Dr. Erdal KORKMAZ
Supervisor

Examining Committee Members

Prof. Filiz GÜNEŞ _____

Assist. Prof. Dr. Erdal KORKMAZ _____

Assist. Prof. Dr. Ali UZER _____

It is approved that this thesis has been written in compliance with the formatting rules laid down by the Graduate Institute of Sciences and Engineering.

Assoc. Prof. Nurullah ARSLAN
Director

DESIGN, ANALYSIS AND IMPLEMENTATION OF NARROW BEAM DIRECTIVE SMALL SIZE ANTENNAS IN 0.5–3 GHz BAND

Ashrf AOAD

Master of Science Thesis – Electrical and Electronics Engineering Department

May 2011

Supervisor: Assist. Prof. Dr. Erdal KORKMAZ

ABSTRACT

Subsurface imaging applications and other applications where the penetration depth, resolution and suitability for multi antenna arrangement are concerned, there is a need for directive antennas operating at relatively low frequencies, having smaller lateral size and narrow radiation pattern. However these requirements are constrained by inverse relationship about the electrical size of the antenna and its operating frequency. The aim of this thesis is to design, analysis, simulation and implementation of small size, to be able to operate at lower frequencies and narrow beam directive antennas.

During the thesis term many antenna types are investigated, however, microstrip antenna is chosen as a template since it has a high performance in many applications due to its lightweight, low profile with conformability and ease of integration in other systems. The antennas are designed and implemented on a dielectric substrate in two rectangular and one circular spiral microstrip shape. An agreement is observed between the measured and simulated results in terms of aimed output.

Keywords: Spiral Microstrip Antenna Design, Microstrip Antenna Simulation, Narrow Beam Small Microstrip Antennas, Low Frequency Microstrip Antennas.

IŞIMA ARALIĞI DAR, YÖNLÜ VE KÜÇÜK BOYUTLU ANTENLERİN 0.5-3 GHZ BANDINDA TASARIMI, ANALİZİ VE GERÇEKLEŞTİRİLMESİ

Ashrf AOAD

Yüksek Lisans Tezi – Elektrik Elektronik Mühendisliği Bölümü

Mayıs 2011

Tez Danışmanı: Yrd. Doç. Dr. Erdal KORKMAZ

ÖZ

Yeraltı görüntüleme ve mikrodalga hipertermi gibi nüfuz derinliği ve çözünürlüğün önemli olduğu uygulamalarda çoklu dizi anten kullanılmasına da imkân sağlamak amacıyla boyutları küçük, ışıma aralığı dar ve düşük frekanslarda da çalışabilen antenlere ihtiyaç duyulmaktadır. Ancak antenin elektriksel uzunluğu ile frekansı arasında bulunan ters ilişki bu antenlerin tasarımını kısıtlamaktadır. Bu tezin amacı boyutları küçük, ışıma aralığı dar, düşük frekanslarda da çalışabilen farklı antenlerin tasarımı, analizi, benzetimi ve üretiminin gerçekleştirilmesidir.

Tez süresi boyunca birçok anten şekli incelenip benzetimleri yapılmasına karşın mikroşerit antenler üretiminin kolay ve ucuz oluşu, uyumluluğu, başka sistemlere entegrasyonu kolay oluşu ve performansının hedeflere uygunluğu nedeni ile tercih edilmiştir. Tasarlanan ve üretilen mikroşerit antenler dielektrik bir taban üzerinde metalik mikroşeritler ile iki karesel ve bir dairesel spiral şeklindedir. Üretilen antenlerin ölçüm ve benzetim sonuçlarının hedeflenen çıktılar ile örtüştüğü gözlenmiştir.

Anahtar Kelimeler: Spiral Mikroşerit Anten Tasarımı, Mikroşerit Anten Benzetimi, Dar Işımalı Küçük Mikroşerit Antenler, Düşük Frekanslı Mikroşerit Antenler.

To my beloved parents, family, sisters, brothers especially my big brother Prof. Dr. Mohammed AWAD for their support, love and patience.

ACKNOWLEDGEMENT

I would like to express my sincere gratitude to my project supervisor Assist.Prof.Dr. Erdal KORKMAZ for his guidance, patience and encouragement throughout the duration of this thesis and before.

In particular, I would like to express my appreciation and lots of thanks to Assoc. Prof. Dr. Korkut YEĞİN from Yeditepe University for his assistance to use the facilities in their microwave laboratory.

Especial thanks to Mr. Bayram ÜSTÜN manager of Üstün Reklam for his assistance to print out the antennas. As well as, Thanks from the depth of my heart to my brother Khaled AWAD.

Last but not least, I take this opportunity to express my deepest thanks to my parents, family, sisters, brothers, and their kids. Without their support, love and encouragement, it would not have been possible to pursue my Master of Science degree study. I sincerely thank them.

TABLE OF CONTENTS

LIST OF TABLES

LIST OF FIGURES

LIST OF SYSMBOLS AND ABBREVIATIONS

MSA	Microstrip Patch Antenna
BW	Bandwidth
HPBW	Half Power Beamwidth
$f_\circ$	Frequency
L	Length of the Microstrip Patch Antenna
W	Width of the Microstrip Patch Antenna
h	Substrate Thickness
tan δ	Loss Tangent of Dielectric Material
V	RF Voltage
D	Directivity
ε_r	Relative Permittivity
ε_{eff}	Effective Relative Permittivity
ΔL	Fringe factor
c	Velocity of Electromagnetic Waves in Free Space
VSWR	Voltage Standing Wave Ratio
PEC	Perfect Electrical Conductor
GPR	Ground Penetrating Radar
MHz	Megahertz
GHz	Gigahertz
$\lambda_\circ$	Wavelength in Free Space
VHF	Very High Frequency
UHF	Ultra High Frequency
RHC	Right Hand Side Circular
LHC	Left Hand Side Circular
RSMSA	Rectangular Spiral Shaped Microstrip Patch Antenna
CSMSA	Circular Spiral Shaped Microstrip Patch Antenna

CHAPTER 1

INTRODUCTION

1.1 BACKGROUND INFORMATION

The applications where the penetration depth, resolution and suitability for multi antenna arrangement are concerned, there is a need for directive antennas operating at relatively low frequencies, having smaller lateral size and narrow radiation pattern. One of these applications is the microwave hyperthermia method in which cancerous cells are exposed to electromagnetic radiation to increase the temperature locally in cancer tissues. The method implies to increase temperature in cancerous cells up to 45ºC by using of the electromagnetic absorption effect in the cancerous tissues. In medical sense, to avoid the multiplication of cancer cells the aim is to increase the temperature in cancerous cells from 37ºC-38°C range to 42ºC -45°C range. Although within these temperature ranges it is not possible to kill the cancerous cells directly, however, the intention is to cure it by damaging cancerous cell's protein build and changing cell construction.

The accomplished investigations demonstrated that high temperature obstructs the cancerous cells evolution and even kills them. The cancerous cells dispositions are weaker than healthy ones; the healthy cells near the cancerous cells are damaged lesser [1-3]. To be able to apply this method, the antenna was planned to integrate in the applicator should satisfy some requirements. It has to be suitable for multi source antenna configuration; radiation pattern should be narrow, lateral size small and be capable to resonate at lower frequencies to ensure enough penetration into the tissues.

A second application is the subsurface imaging where the Ground Penetrating Radar (GPR) is used. The GPR has an antenna system which sends electromagnetic wave(s) into the ground and receives back the reflections from the different layers of ground. Each reflection indicates an inhomogeneity in the ground. At single point sending and receiving of signals is called a-scan, keeping the a-scan on a line with a certain displacement is called b-scan and to make a grid with multiple b-scans is called c-scan. To obtain 2D subsurface image b-scans are performed and its reflection pattern is depicted in time domain. If an object is present in the ground, it disrupts the homogeneity in the ground and that is why a curve in time domain reflection diagram is observed. In a similar way c-scans are used to reconstruct 3D subsurface image [4-7].

The efficiency of such an array system to obtain a c-scan at once on a certain region depends strongly on the characteristics of the antennas to be used. To increase the resolution the inter distance between the antennas should be smaller, to have enough penetration, it should be able to operate at lower frequencies and to increase the resolution and decrease the cross coupling the antennas should have a narrow radiation beam.

1.2 PROBLEM STATEMENTS AND AIM OF THE THESIS

Unfortunately the requirements mentioned for such antennas are constrained by inverse relationship about the electrical size of the antenna and its operating frequency. For these reasons the motivation was to investigate whether is it possible to design an antenna which is also capable to operate at relatively lower frequencies (1-3 GHz), have narrower beam width (HPBW < 90°), have no side lobes (directivity about 6 dBi) and have a lateral size smaller than 5 cm. The aim of this thesis is to design, analysis, simulation and implementation of three antennas satisfying the requirements mentioned.

1.3 WORK SCOPE

The first point to be investigated was which antenna template to choose and design the antennas. For that purpose many antenna types are investigated, designed and simulated. However, in this thesis only the results of chosen best three antennas are presented. After evaluation of the survey the microstrip patch antenna (MSAs) is chosen as a template since they have significant number of advantages over

conventional antennas such as low profile, lightweight, conformability, low production cost and easy fabrication properties using modern printed-circuit technology [8, 9].

The microstrip patch antenna is usually reconfigured to design new forms in order to satisfy the requirements in different applications. Reconfigurable MSA's received great attention in wireless communication systems due to their selectivity for operating frequency, pattern and polarization [10]. Reconfiguration of antennas has a feature in operating more than one frequency and narrow bandwidth also observed in our results which depends on the formation of a new shape of antenna.

In this thesis the microstrip antenna is reconfigured to take a new microstrip spiral patch form. The new pattern is combined between the shape of Archimedean spiral and microstrip antenna. They obey the characteristics and advantages of both of them. The main elements in the production and fabrication of MSA's are a metallic patch and a substrate where the patch is grounded on the substrate. The metallic patch can take and reconfigure in many different forms such as rectangular and circular to design new reconfigured structures. The antennas consist of three layers over each other, by assuming the first layer is metallic, the second is substrate with dielectric material and the last layer will be the ground which is a metallic and used as a reflector and director. The differences of the structure of antennas are in the size and the substrate material, where the vacuum is used in the larger antenna and Rogers RT 5880 (lossy) in others as a substrate material. The MSA's have narrow bandwidth especially for substrates greater than $0.02\lambda_0$ where λ_0 is the wavelength in the free space.

1.4 OUTLINE OF THESIS

Chapter 2 presents the basic theory of spiral and microstrip patch antennas including fundamental geometries, advantage and disadvantages. Chapter 3 provides the literature review relating to the designed antennas. In addition to the formulas used to calculate the sizes of antennas and which methods are used to reduce the sizes. The relationship is also reviewed between the spiral and microstrip patch antennas. Theoretical analysis between simulated results and calculated. Chapter 4 includes the conclusion of the thesis and a summary of work.

CHAPTER 2

THEORY OF MICROSTRIP PATCH AND ARCHIMEDEAN ANTENNAS

2.1 INTRODUCTION

All antennas share the same property in transmitting and receiving electromagnetic waves in free space at a wide range of frequencies. Typically consist of a metallic conductor and dielectric layer. The combining between the microstrip patch and Archimedean spiral properties in the shape of the designed antenna make us to introduce both of them in this chapter.

2.2 MICROSTRIP PATCH ANTENNA

It has been classified as a newer technology to the world of antenna and propagation engineering. This stems from factor of performance in applications. Indeed, the microstrip antenna is the one of many antennas type can be reconfigured to generate new forms. In addition, microstrip antennas also exhibit large electromagnetic signatures at certain frequencies outside the operating band, are rather large physically at VHF and possibly UHF frequencies, and in large arrays there is a trade-off between bandwidth and scan volume [11, 12].

The two types of the microstrip patch antenna that reconfigured, designed, simulated, analyzed and fabricated are rectangular and circular.

2.2.1 Rectangular Microstrip Patch Antenna

The rectangular patch is by far the most widely used configuration. It is very easy to analyze using both the transmission-line and cavity models, which are most accurate for thin substrates [13]. The rectangular microstrip patch antenna (RMPA) is the first reconfigured antenna in the thesis.

2.2.2 Circular Microstrip Patch Antenna

The next most popular configuration is the circular patch. It also has received a lot of attention not only as a single element [14], but also in arrays [15].

As far as, the control into the rectangular patch is being with width *W* and length *L* and the ratio between them, the circular has radius of patch as well.

2.3 ARCHIMEDEAN SPIRAL ANTENNA

It has been ranked as an ideal antenna to use for many communication systems, where many frequencies are monitored at once. In fact the spiral antenna has a feature and a technique to generate new shapes. As well as spiral antennas belong to the class of frequency independent antennas which operate over a wide range of frequencies. Polarization, radiation pattern and impedance of such antennas remain unchanged over large bandwidth [16]. Spiral antennas are useful for finding microwave direction [17].

2.4 BASIC CHARACTERISTICS

The basic geometry of the antennas is metallic and dielectric substrate; the metallic parts are feeding, strip and a ground. The metallic patch is normally made of thin copper foil or is copper-foil plated with a corrosion resistive metal, such as gold, tin, or nickel. Where the dielectric constant is ε_r usually in the range of $2.2 \leq \varepsilon_r \leq 12$ and thickness is h, as shown in Figure 2.1. The following explanation of antennas are the most usable that I have used in my thesis.

2.4.1 Geometry of Microstrip Patch Antennas

They have most commonly shapes like rectangular and circular. These patches have been using for the simplest and the most demanding applications as illustrated in Figure 2.1. There are other types of radiating patch configurations such as square, dipole, elliptical, triangle, shapes of English letter or any other forms. According to the freedom in the *xy* plane gives rise to the possibility of a multiplicity of a possible shapes. Only a few have been seriously examined such as the rectangular or square patch and disc [18]. Microstrip antennas consist of a very thin patch printed on the top of substrate, ground also printed on the down of substrate. The most important dimensional parameters in microstrip circuit design are the width *W* and height *h* (equivalent to the thickness of the substrate) [19].

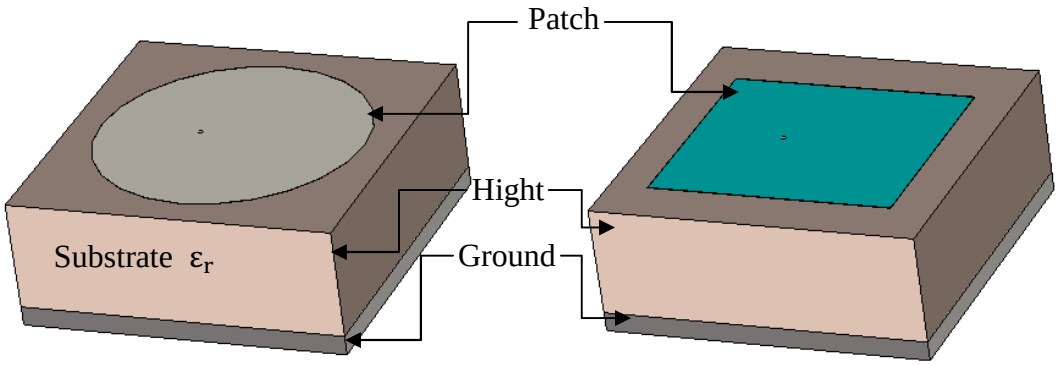

a. Circular b. Rectangular

Figure 2.1 Representative two shapes of Microstrip patch elements

2.4.2 Geometry of Archimedean Spiral Antennas

Which consist of a tight coil that circles around in either a clockwise or counter-clockwise direction on grounded dielectric substrate and also have different number of arms usually two or four to radiate in multiple modes or to suppress unwanted modes. Some types of Archimedean spiral antennas are mentioned here like circular, square and hybrid, in some cases the cavity plays an important role to exhibit higher order resonances. Archimedean spiral antennas have received and increased interest due to their wide bandwidth [20], high efficiency, low profile, stable impedance characteristic and circular polarization over the last two decades. Since the structure is rotationally

symmetric, the pattern is also nearly rotationally symmetric. The polarization of the radiated field is very close to circular in all direction, with the sense determined by the sense of the spiral. I have just defined two shapes of them as in Figure 2.2 that similar with simulated antennas in this thesis.

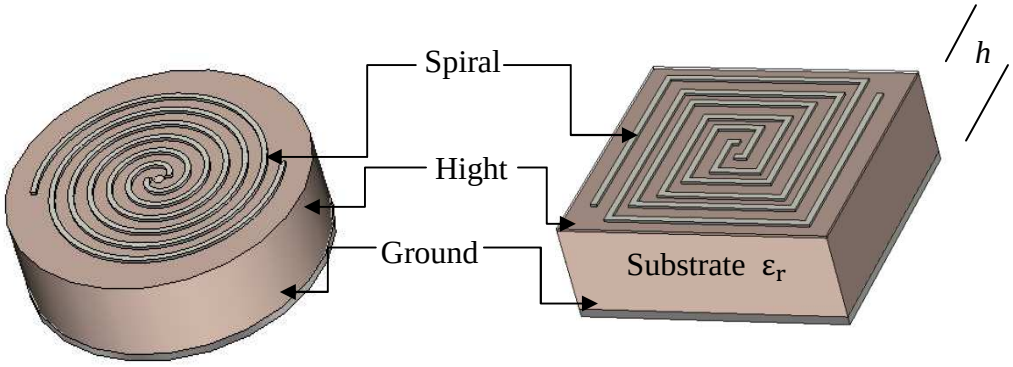

a. Circular Archimedean b. Rectangular Archimedean

Figure 2.2 Representative two shapes of Archimedean spiral elements

2.5 FEEDING METHODS

2.5.1 Feeding of Microstrip Patch Antennas

Microstrip Patch Antennas may fed by one of four configurations. The four most popular are the microstrip line, coaxial probe, aperture coupling, and proximity coupling [21, 22]. To select a technique of feedings, it must be taken into account a number of factors. The most important consideration is the efficient transfer of power between the radiating structure and feed structure, that is, impedance matching between the two. Associated with impedance matching are stepped impedance transformers, bends, stubs, junction, transitions, and so on. In this thesis only the practical types of feeding will be covered which interest to the designer.

The coaxial line or probe that composed of two cylinders, the inner is from the perfect electric conductor PEC, the outer is connected to the ground plane. It also has a narrow bandwidth.

2.5.2 Feeding of Spiral Antennas

In the spiral antenna, the feeding system also is multiple, balun, infinite balun, beam former and coaxial line feed. Because the designer has used the coaxial line for the simulated antennas, the explanation will be just about it. Where displayed in Figure 2.3 a. and b. a set of equivalent electronic circuit.

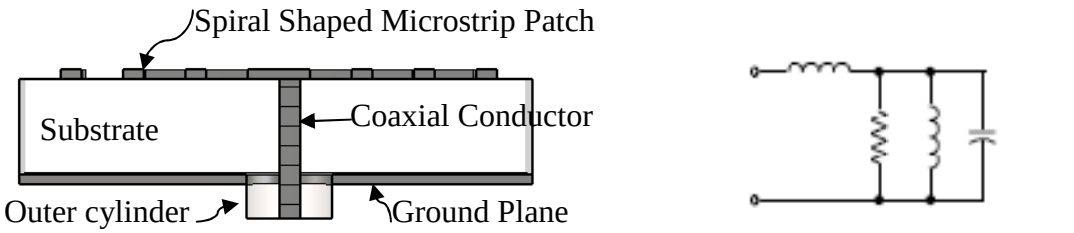

a. Probe feed. b. Probe electronic circuit

Figure 2.3 Representative probe feed and equivalent electronic circuit

2.5.3 Probe Electronic Circuit

The circuit consists of electronic elements, inductance, reactance, resistance and power supply as shown in Figure 2.3.b. this circuit is found and connected to the input of the feeding system to supply electrical energy, in this process, the impedance is produced as an ohmic value. Many important factors locate the impedance value as well. The input impedance for a probe excited microstrip antenna can be calculated and defined by started by

$$Z_{in} = V/I_s \tag{2.0}$$

Where V is the RF voltage across the probe and I_s in the probe or source current. I_s can be chosen to be 1A. There are also many formulas to locate the place of feeding point and support the calculations, in the formulas the width W, length L and height h of substrate must be taken into account.

Typically the feed reactance is very small, compared to the resonant resistance, for very thin substrates. However, for thick elements the reactance may be significant and needs to be taken into account in impedance matching and in determining the

resonant frequency of a loaded element [23]. In our thesis the feeding is in the midpoint of structured antenna as presented in the next chapter.

The table below displays the advantages of coaxial probe of feeding system and also the most convenient in our project of antennas design that the designer has preferred.

Table 2.1 Characteristics of the different feeding systems[24]

No	Characteristic	Microstrip line feeding	Coaxial feed	Aperture coupled feed	Proximity coupled feed
1.	Spurious feed radiation	More	Low	Less	Minimum
2.	Reliability	Better	Poor due to soldering	Good	Good
3.	Ease of fabrication	Easy	Soldering and drilling needed	Alignment required	Alignment required
4.	Impedance matching	Easy	Easy	Easy	Easy
5.	Bandwidth	2-5%	2-5%	2-5%	13%

2.6 SUBSTRATE

The first step in the antenna design is to choose an appropriate dielectric substrate with a suitable thichness h and loss tangent δ_s. The value of dielectric constant ε_r and thickness play a role to influence to the results positively or negatively. For example, a low value of substrate constant ε_r will increase the fringing field at the patch and thus the radiated power. Therefore, the preferred value of substrate is $\varepsilon_r \leq 2.5$ unless a smaller size of patch was desired. In other word, the increasing in substrate thickness

value means the decreasing in the value of the dielectric constant ε_r. If the loss of tangent δ_s is high the dielectric will be increased therefore reduce antenna efficiency. Depending on that, a rectangular patch antenna stops resonating for substrate thicknesses greater than $0.11\lambda_\circ$ ($\varepsilon_r = 2.55$) due to inductive reactance of the probe feed [25].Various substrates can be selected and used, but there are most commonly substrate materials with different dielectric value. The place of substrate is visible in Figures 2.1, 2.2, and 2.3.

Archimedean spiral antenna subjects to the same conditions in the selection of substrate materials.

Generally, substrate materials [26] can be separated into three categories in accordance with their dielectric constant:

1. Having a relative dielectric constant (ε_r) in the range of 1.0–2.0. This type of material can be air, polystyrene foam, or dielectric honeycomb.
2. Having ε_r in the range of 2.0–4.0 with material consisting mostly of fiberglass reinforced Teflon.
3. With an ε_r between 4 and 10. The material can consist of ceramic, quartz, or alumina.

2.7 GROUND PLANE

Ground plane sizes divided into two parts infinite and finite. Here I will just explain the finite size which is used in the simulated antennas. For the use of microstrip antenna as a reflector feed, the ground plane dimensions should be limited, if the goal is to reduce the antenna size and the ground plane extension beyond the patch dimensions to minimum. Finite ground plane gives rise to diffraction of radiation from the edges of the ground plane resulting in changes in radiation pattern, radiation conductance, and resonant frequency. Kuboyama et al. have reported the results of experimental investigations on the resonant frequency, radiation pattern, and gain of a rectangular patch as a function of ground plane size [27]. It was found that for a patch antenna with the ground plane size equal to the patch metallization. It has been also found a finite

ground plane gives rise to scattered radiation in the backward direction. The place of ground plane is visible in Figures 2.1, 2.2, and 2.3.

2.8 METHODS OF ANALYSIS

2.8.1 Description of the Transmission Line Model

The transmission line will be discussed only for rectangular and circular microstrip antennas. The most popular models for analysis of microstrip patch antennas are the transmission line model, cavity model, and full wave model [28]. The transmission-line model is the easiest of all, it gives good physical insight, but is less accurate and it is more difficult to model coupling [29]. In this chapter I will cover the transmission line only. In designed and simulated model, the microstrip antenna is modeled as a length of transmission lines of characteristic impedance $Z_\circ$ and propagation constant $\gamma = \alpha + j\beta$, where β is the phase of constant. The field vary along the length of the patch, which usually a half-wavelength, and remain constant across the width. Radiation occurs mainly from the fringing fields at the open ends. The probe fed-patch radiator along with the transmission line equivalent circuit is shown in Figure 2.3 b. Input impedance of the patch antenna based on this equivalent circuit is easily obtained as $Z_{in} = jX_L + Z_1$ where X_L is the probe reactance and $Z_1 = 1/Y_1$.

2.8.2 Fringing Effects

In the finite edges of the patch dimension along the length and width, the field at the edges of the patch undergoes fringing. This is clearly shown at the length L and width *W* of the patch for two radiating edges as shown in Figure 2.4. For E plane (x-y plane) fringing is a function of the ratio between the length *L* of the patch and the height *h* of substrate (*L/h*) and the dielectric constant ε_r. Since *L/h* and *W/h*$\gg$ 1, fringing is reduced. The electric field lines concentrate mostly in the substrate. Fringing in this case makes the microstrip line look wider electrically compared to its physical dimensions. Since some of the waves travel in the substrate and air, an effective dielectric constant ε_{reff} is introduced to account for fringing and the wave propagation in the line [30]. For low frequencies the effective dielectric constant is essentially

constant. At intermediate frequencies its values begin to monotonically increase and eventually approach the values of the dielectric constant of the substrate [30].

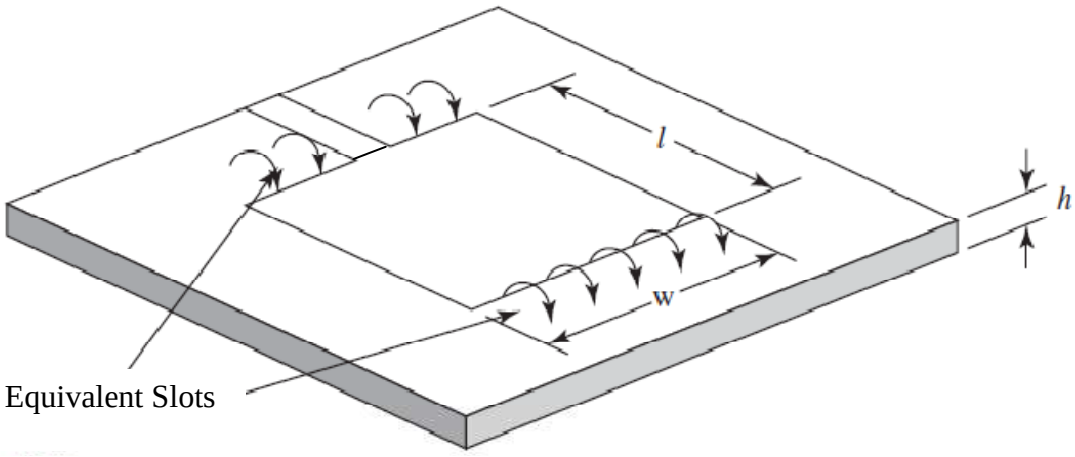

Figure 2.4 Microstrip patch radiation source represented by two equivalent slots

2.8.3 Radiation and Directivity

The radiation comes from the fringing fields at the two open ends, as discussed above, which is equivalent to two slot antennas separated by a distance *L* as shown in Figure 2.4. The radiation patterns in the two principal planes are E-plane $\emptyset = 0°$ and H-plane $\emptyset = 90°$.

A spiral radiates RHC (Right Hand side Circular) polarization on one side and LHC (Left Hand side Circular) polarization on the other side.

The radiation patterns are not sensitive to the resonant frequency or the size of the patch, the results to be presented are obtained by side length *L*. as shown in Figure 2.4.

With the radiated field, the directivity able to be computed using equation:

$$D_O = \frac{4\pi U}{P} \tag{2.1}$$

Where *P* the total is radiated power in *W* and *U* is the radiation intensity in W/unit solid angle.

Asymptotically, the directivity of the microstrip antenna can be expressed as:

$$D = \begin{cases} 6.6 = 8.2\ dBi, & W \ll \lambda_\circ \\ \dfrac{8W}{\lambda_\circ} & W \gg \lambda_\circ \end{cases} \quad (2.2)$$

The larger the width, the larger the directivity. These are approximations as well; the actual directivities are slightly lower than these values [31].

In the next chapter which relates to the design, calculation and simulation of antennas, the equation (2.2) will be taken as a reference expression of the directivity values.

2.9 ADVANTAGE AND DISADVANTAGE

There are advantages as well as disadvantages associated with the microstrip patch antenna.

The advantages are:

1. Extremely low profile lightweight and low cost.
2. Simple in fabrication process.
3. Generally has a narrow bandwidth.
4. Easily integrated with microwave integrated circuits.
5. Capable of dual and triple frequency operations.

The disadvantages of the microstrip antennas are the following:

1. Narrow bandwidth
2. Low efficiency
3. Low gain
4. Extraneous radiation from feeds and junctions
5. Low power handling capacity
6. Surface wave excitation

2.10 CONCLUSION

In this chapter, a general method has been presented that includes the classification and geometries of two types of microstrip patch and Archimedean spiral antennas, the circular, rectangular and spiral were studied in some details such as figures and descriptions. On the other hand, the feed point location was shown to influence resonant modes. In addition, it was shown by selecting an appropriate substrate and ground-plane size, nearly radiation patterns and directivity.

CHAPTER 3

DESIGN AND SIMULATION PROCEDURES OF SPIRAL SHAPED MICROSTRIP PATCH ANTENNAS

3.1 INTRODUCTION

The objective in this chapter is to introduce a process to design and simulate the desired antennas by calculated characteristics. The proposed design process is composed of several steps, started by calculated dimensions through several different steps ended by obtained results. As a typical antenna, I will design, analyze and implement the three types of microstrip patch antenna sequentially. The ways have been taken to combine and reconfigure the patch and spiral antennas which shall be presented as well. The difference and variance also between the designed and simulated antennas will be discussed by figures, mathematical formulations, utilized materials and the dimensions. In addition to theory of, try and error, to improve and access to the best results.

The types of discussed antennas are rectangular and circular spiral shaped microstrip antennas with the variety in sizes. All designed antennas in this chapter are single.

The coaxial feed position is determined at the center of the antennas and adjusted to give optimal matching ~50 ohm (characteristic impedance) at the port.

3.2 THE FIRST ANTENNA : RECTANGULAR SPIRAL SHAPED MICROSTRIP PATCH ANTENNA 10x10.5 CM

3.2.1 Substrate Selection

The first design step is to choose a suitable dielectric substrate of convienent thichness h and loss tangent. The used substrate materials were vacuum with $\varepsilon_r = 1$ and *h*=2. 69 cm. the frequency ranged from 500 MHz to 3 GHz, to calculate center frequency,

$$f_r = \sqrt{f_1 f_2} = \sqrt{0.5 * 3} = 1.225 \text{ GH} \quad (3.0)$$

To meet the goal of a broadband antenna, Where f_r is the center frequency.

3.2.2 Width and Length of RSMPA 10x10.5 cm

The following information was taken into account through selecting the physical dimension of antennas.

Patch width affects the input resistance and bandwidth to a larger extent. It has a minor effect on the resonant frequency and radiation pattern of the antenna. A larger patch width increases the power radiated and thus gives decreased resonant resistance, increased bandwidth, and increased radiation efficiency.

In this design, a length *L* often greater than the width *W* without exciting undesired modes, the procedure of design assumes that the specified information includes the dielectric constant of the substrate ε_r, the resonant frequency f_r, and the height of the substrate *h*.

As it was mentioned previously, the aim of this design was to have small size, low frequency and narrow beam. Thus let me starting with assuming and analyzing the followings:

3.2.3 First Case

In the first case the basic microstrip patch antenna is represented with Width *W= 1 cm*, Length *L= 1.5 cm,* and this is the first assuming to obtain low frequency that is one

aim of many in this thesis. The metallization patch dimensions are smaller than substrate dimension by 0.5 cm of each edge.

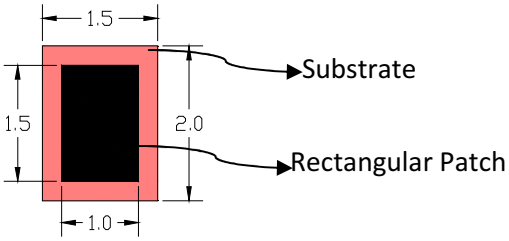

Figure 3.1 Experimental model of mid part of rectangular patch antenna.

By the following formula, the resonant frequency may be calculated.

$$f_0 = \frac{c}{2W\sqrt{\frac{\varepsilon_r + 1}{2}}} \tag{3.1}$$

Where the *c* is the free-space velocity of light, *W*= 1 cm and $\varepsilon_r = 1$

$$f_0 = \frac{30}{2 * 1\sqrt{\frac{1+1}{2}}} = 15 \text{ GHz} \tag{3.1a}$$

After doing the calculation and simulation using the sizes shown on the Figure 3.1 and resulted frequency in (3.1a), we have found the required conditions have not been achieved.

Accordingly, The value of f_0 is not low. Therefore, it is not acceptable. After doing some reconfigurations in many experimental models by adjusting sizes to get the desired. I have reached to conclusion; the best way is to do approximation for adding followed arms to the rectangular patch to affect in reducing the frequency value from higher value $f_0 = 15$ GHz to lower and to improve the far field pattern with directivity and narrow beam.

The simulated resonant frequencies are 1.5256 GHz, 5.594 GHz, and 11.357 GHz (See Appendix A).

3.2.4 Second Case

Thus, in the second case of experimental modes, that by configuring the rectangular patch by adding first turn of microstrip patch with 90° to each coiled arm in the directions (+,-) signs, the total angle of a coil is 360°, increasing 0.5 cm in every arm of the coil, to become as shown in Figure 3.2, with a note that the height *h*, and the material of substrate are constant.

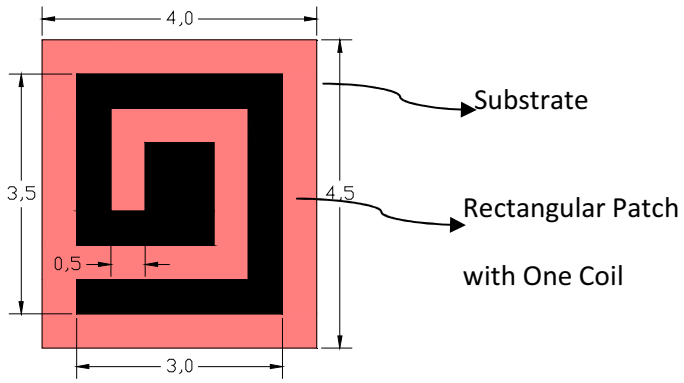

Figure 3.2 Experimental model of rectangular patch antenna with one angular coil

As shown in the Figure 3.2 the width *W*=3cm, with the observation, the free space between the mid microstrip patch and the first coil that is not considered into the calculations bellow.

$$f_0 = \frac{30}{2 * 3\sqrt{\frac{1+1}{2}}} = 5 \text{ GHz} \qquad (3.1b)$$

Let us analyze the result of f_0 = 5 GHz in equation (3.1b) with making a comparison with the value of the frequency in the first case. We will find that, whenever the width of antenna increases the resonant frequency decreases. In both cases, the simulation of the antenna's radiation pattern in the far field region was worse, and the resonant frequency was multiple.

According to the shape above, we can clearly see that the form has started to take spiral shape bit by bit.

The simulated resonant frequencies are 0.576 GHz, 1.485 GHz, 7.672 GHz, and 11.364 GHz (See Appendix A).

3.2.5 Third Case

The calculated and simulated results in the second case prompted me to reconfigure the patch by adding second angular coil under same conditions explained previously. Width *W= 5* cm, Length *L= 5.5* cm.

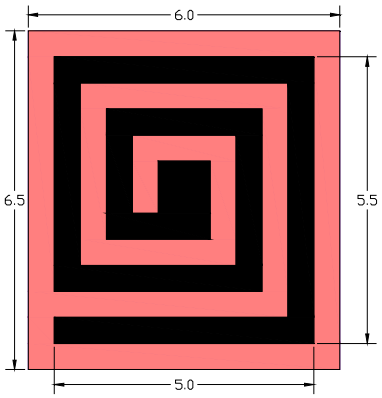

Figure 3.3 Experimental model of rectangular patch antenna with two angular coils

$$f_0 = \frac{30}{2 * 5\sqrt{\frac{1+1}{2}}} = 3 \text{ GHz} \qquad (3.1c)$$

From the calculated results, it seems that we approach to obtain good results (low frequency with small sizes, as it was needed). But the simulation outputs appeared vice that the s-parameters were good, but the far field pattern has worse consequences. So I have to add an angular coil more to be the third angular coil.

The simulated resonant frequencies are 0.2611 GHz, 0.759 GHz, 6.418 GHz, and 12.057 GHz (See Appendix A).

3.2.6 Fourth Case

After adding the third angular coil through increasing the width *W=7* cm, length *L=7.5* cm and the evaluated resonant frequency from the equation (3.1d) is 2.1 GHz. From the summery Table 4.3 it could be seen obviously the difference between the evaluated value in equation (3.1d) and the resulted values in the design software.

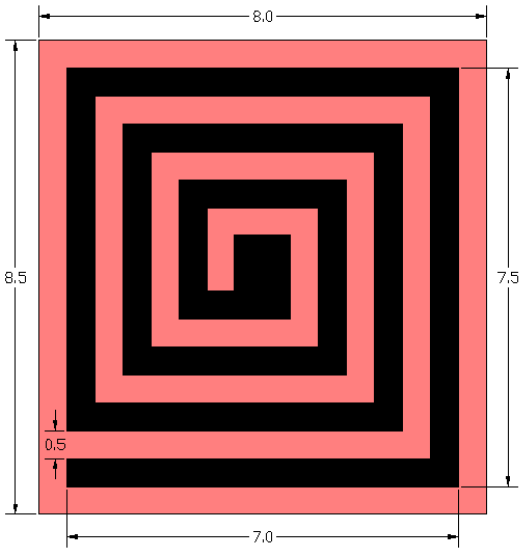

Figure 3.4.1 Experimental model of rectangular patch antenna with three angular coils

$$f_0 = \frac{30}{2 * 7\sqrt{\frac{1+1}{2}}} = 2.1 \text{ GHz} \qquad (3.1d)$$

The simulation of Figure 3.4.1 has outputted two resonant frequencies, the first at 0.96 GHz and the other is at 1.16 GHz. While f_0 at 0.96 GHz has a worse value of the far field and directivity, but f_0 at 1.16 GHz has a good value for the far field and directivity. As summarized in the Table 3.1.

Table 3.1 Summary of simulated results in fourth case of RSMPA without reflector

No	f_0 (GHz)	S-Parameters	Directivity (dBi)	VSWR	HPBW	Side lobe level (dB)
1.	0.9582	-8.565	worse	1.278	worse	no
2.	1.1626	-18.261	7.519	2.18	37.3°	-7.3

Where phi (Ø) =90°, there is a main lobe direction value of 1° at f_0=1.1626 GHz.

According to the equation 2.2 and its condition into chapter 2, all visible results of directivities “D” in the summery Table 3.1 are actual values.

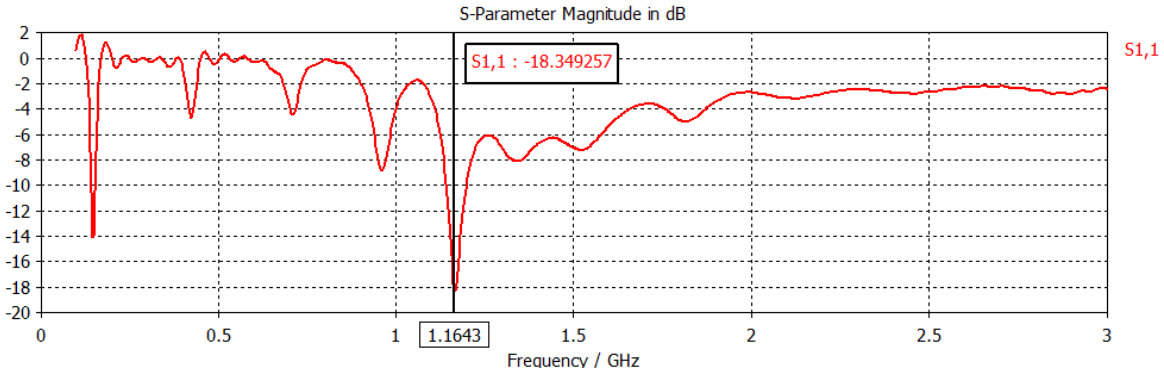

Figure 3.4.2 S11-Parameter for rectangular spiral shaped microstrip antenna without reflector

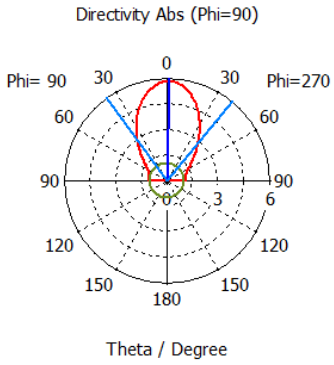

Figure 3.4.3 Two dimensional far field pattern (in linear scale) at frequency 1.1626 GHz

From sequence of cases above, the improvement of results has been noted clearly, so in the next case, the added arm will be the reason of investigation of improvements that desired and focused onto shifting of resonant frequencies to be lower than was found in the Table 3.4 and fourth case.

3.2.7 Fifth Case

This is the final case of shape which has verified in the form and dimensions shown in Figure 3.5.1. A separated and closed rectangular coil will be added to the shape of antenna. In other words, the formatted shape is a rectangular spiral shaped microstrip patch antenna (RSMSA) with a reflector. The reflector has same dimension in the height 0.269 cm and a distance away 0.5 cm evenly from all edges of spiral shaped patch antenna which is exciting in the middle. The total length of the turned microstrip is 65 cm, besides the reflector dimension $L_r * W_r$ as 9.5 x 9 cm.

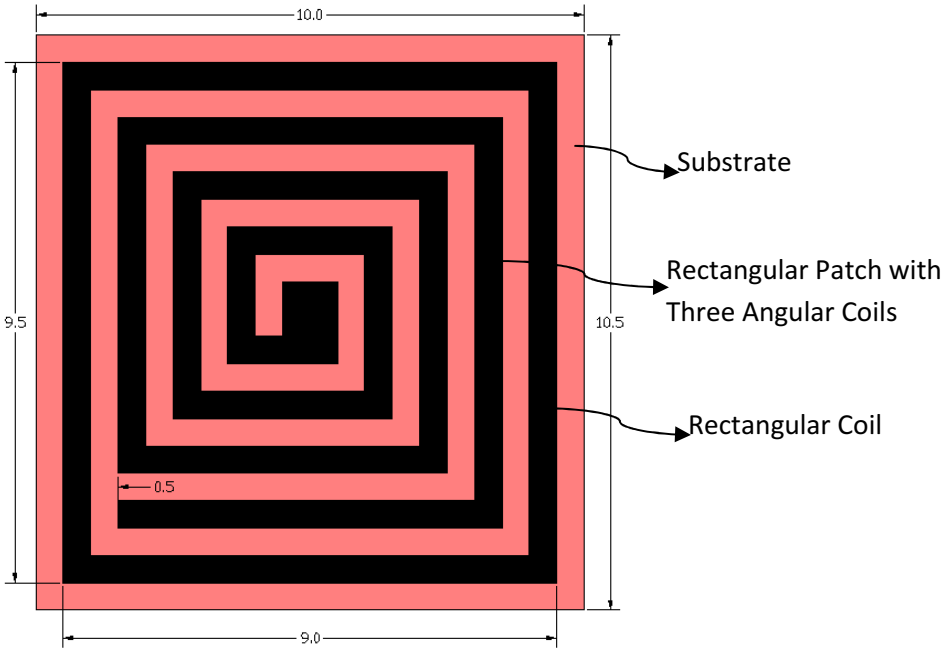

Figure 3.5.1 Experimental model of rectangular spiral patch antenna with three angular coils and reflector

This is the final required designed and simulated an antenna shape with the dimensions shown on the design above.

$$f_0 = \frac{30}{2 * 9\sqrt{\frac{1+1}{2}}} = 1.6 \text{ GHz} \qquad (3.1e)$$

The calculated resonant frequency in the above formula (3.1e) with the value of width *W* shown on Figure 3.5.1 is larger than simulated, but it is at the range that is needed and aimed.

So, from the calculated values in the following equations, the shown outputs will be approximated to have the optimum. Based on the simplified formulation that will be described, a design procedure outlines and leads to practical designs of dimension of rectangular microstrip patch antenna with taken the changing and reconfiguring in the shape of antenna into account, and also the empty areas between arms.

1. At $f_r = 0.884$ GHz, W=9 cm = 0.2652 λ, h=2.69 cm = 0.079 λ, and $\varepsilon_r = 1$.

To determine the effective dielectric constant:

$$\varepsilon_{reff} = \frac{\varepsilon_r + 1}{2} + \frac{\varepsilon_r - 1}{2}\left[1 + 12\frac{h}{W}\right]^{-1/2} \tag{3.2}$$

Under the condition, $W / h > 1$, ε_{reff} may be calculated by:

$$\varepsilon_{reff} = \frac{1 + 1}{2} + \frac{1 - 1}{2}\left[1 + 12\frac{2.69}{9}\right]^{-1/2} = 1 \tag{3.2a}$$

To find L, firstly ΔL should be calculated using:

$$\Delta L = 0.412 * h\frac{\left(\varepsilon_{reff} + 0.3\right)\left(\frac{W}{h} + 0.264\right)}{\left(\varepsilon_{reff} - 0.258\right)\left(\frac{W}{h} + 0.8\right)} \tag{3.3}$$

With substituted the values of W, h, and ε_{reff}, the obtained is:

$$\Delta L = 0.412 * 2.69\frac{(1 + 0.3)\left(\frac{9}{2.69} + 0.264\right)}{(1 - 0.258)\left(\frac{9}{2.69} + 0.8\right)} = 1.691 \tag{3.3a}$$

The actual length L of the patch is found using:

$$L = \frac{\lambda}{2} - 2\Delta L \tag{3.4}$$

Where $\sqrt{\mu_\circ \varepsilon_\circ}$ yielded to 1, the L will take several values at each resonant frequency, thus L is:

$$L = \frac{30}{2 * 0.884\sqrt{1}} - 2 * 1.691 = 13.586 \text{ cm} \quad (3.4a)$$

Finally the effective length L_e is:

$$L_e = L + 2\Delta L \quad (3.5)$$

By substituting (3.3a) and (3.4a) in (3.5) the result of L_e is:

$$L_e = 16.968 \text{ cm} \quad (3.5a)$$

2. At $f_r = 0.954$ GHz, W=9 cm = 0.2862 λ, h=2.69 cm, and $\varepsilon_r = 1$.

With the notation, the values of ε_{reff} and ΔL will be as computed in (3.2a) and (3.3a) respectively. Thus from (3.4) we find

$$L = \frac{30}{2 * 0.954\sqrt{1}} - 2 * 1.691 = 12.341 \text{ cm} \quad (3.4b)$$

From the (3.5), the effect length L_e is:

$$L_e = 15.723 \text{ cm} \quad (3.5b)$$

3. At $f_r = 1.154$ GHz, W=9 cm = 0.3462 λ, h=2.69 cm, $\varepsilon_r = 1$.

With the notation, the values of ε_{reff} and ΔL will be as computed in (3.2a) and (3.3a) respectively. Thus from (3.4) we find:

$$L = \frac{30}{2 * 1.154\sqrt{1}} - 2 * 1.691 = 9.616 \text{ cm} \quad (3.4c)$$

From the (3.5), the effect length L_e is:

$$L_e = 12.998 \text{ cm} \tag{3.5c}$$

According to *W*=9cm, f_r changeable, *h*=2.69 cm, and $\varepsilon_r = 1$. L has normally different values as shown in the equations (3.4a, b, c) and (3.5a, b, c), which dependants on the changing in resonant frequency makes changing in the dimension of the patch.

When the design has been simulated by the obtained values, the results were not acceptable. So the optimum case is in approximating and selecting *W*=9cm, and *L*=9.5 cm, as shown on the Figure 3.5.1.

Through the analytical cases above, we found that the antenna collected in the shape bit by bit between the spiral and microstrip patch, with taking the characteristics of each of them.

The above formulations were theoretically from the patch mathematical equations, the following formulations will be also theoretically, but from spiral mathematical equations, with reference to the spiral shaped patch in the Figure 3.5.2 as a reference:

Firstly, two circles should be drawn as shown in the Figure 3.5.2, to achieve that, I have fixed the center of circles onto the center of feeding which is over the center of microstrip.

Secondly, the small circle must be touched the upper edges of microstrip with radius 0.7 cm, the lager circle also touched the inner edges of a reflector with radius 5.7 cm.

Finally, it is not important if the diameters of circles differ a little bit in the value, because the process depends on the approximation in selecting the diameters of inner and outer circles.

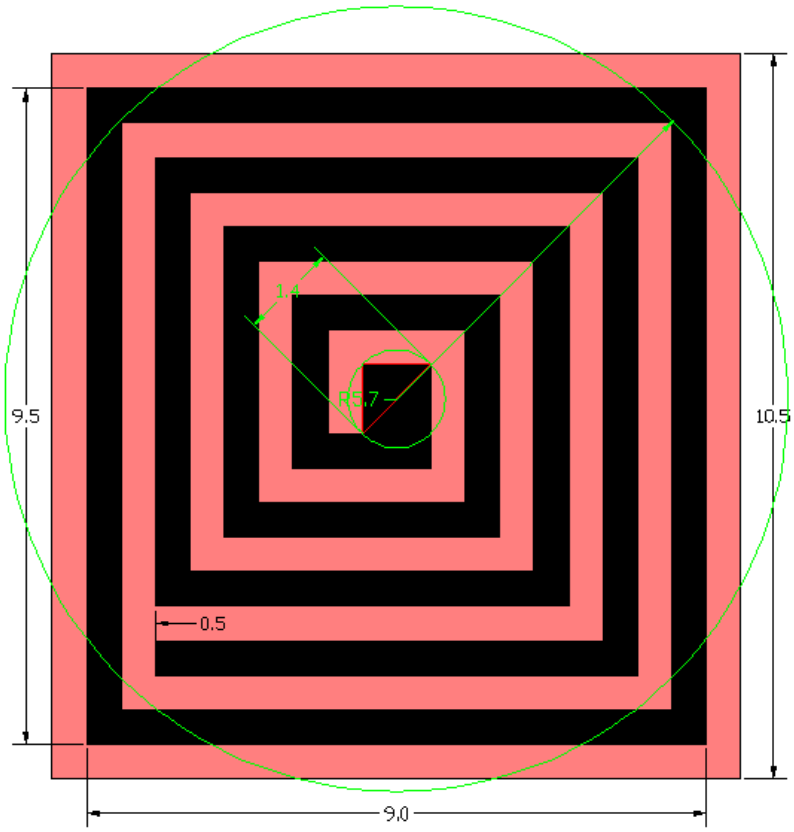

Figure 3.5.2 Experimental model of rectangular spiral patch antenna with three angular coils and reflector

The low frequency operating point of the spiral is determined theoretically by the outer radius and given by

$$f_{low} = \frac{c}{2\pi r_2} \tag{3.6}$$

Where inner radius $r_1 = 0.7$ cm, outer radius $r_2 = 5.7$ cm and c the speed of light.

Thus,

$$f_{low} = \frac{30}{2\pi * 5.7} = 0.837 \text{ GHz} \tag{3.6a}$$

The high frequency operating point is based on the inner radius and given by

$$f_{high} = \frac{c}{2\pi r_1} \tag{3.7}$$

Thus,

$$f_{high} = \frac{30}{2\pi * 0.7} = 6.82 \text{ GHz} \quad (3.7a)$$

The result of low frequency is very close to the result obtained through simulation as shown into summery Table 2.3.

3.2.8 Characteristic Impedance

Under the condition, W_0/ h < 1, where $W_0 = 0.5$ cm is the width of the microstrip line and $\varepsilon_{reff} = 1$, Z_0 may be calculated by:

$$Z_0 = \frac{60}{\sqrt{\varepsilon_{reff}}} \ln\left[\frac{8h}{W_0} + \frac{W_0}{4h}\right] \quad (3.8)$$

This Z_0 formula can effectively match characteristic impedance of the patch antenna.

$$Z_0 = \frac{60}{\sqrt{1}} \ln\left[\frac{8x2.69}{0.5} + \frac{0.5}{4x2.69}\right] = 225\ \Omega \quad (3.8a)$$

As obtained by equation (3.8a) Z_0 is strongly dependent upon the substrate height, width, and ε_{reff} . But there is a different between the result in equation (3.8a) and simulated value of Z_0 by CST MICROWAVE software, where $Z_0 = 50.96\ \Omega$ which was evaluated by adjusting the radius of inner and outer cylinders of the probe in the feeding system, as shown and explained in chapter 2.

The simulation of the model in Figure 3.5.1 has outputted the good result compared with the model in the previous cases. In addition to achieve the desired aims of the design, low frequency, small size and narrow beam.

As mentioned earlier, the design and simulation process was to design and simulate a single reconfigured microstrip patch antenna to be formed as a spiral shape.

After the rectangular antenna model simulated using the final shape shown Figure 3.5.1. The following item displays the results and analysis of the design.

3.2.9 Results

The magnitude of S_{11} versus frequency (also referred to as return loss) is shown, as a verification of the design, in Figure 3.6. It shows the rectangular spiral shaped microstrip patch antenna is as good as resonating at multiple frequencies 0.884, 0.954 and 1.1542 GHz with also multiple return losses -12.731 dB, -14.774 dB and -27.316 dB, and their -10 dB bandwidths are 0.014465 GHz, 0.03317 GHz and 0.051714 GHz, respectively.

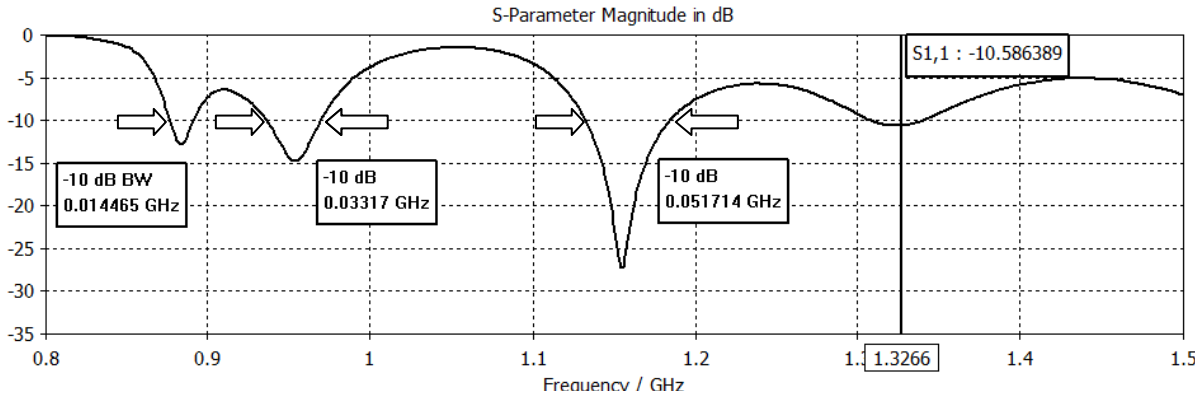

Figure 3.6 S-Parameters for resonating frequencies for 10x10.5 cm of RSMPA

To have stable and stricter values of VSWR, the recommended bandwidth of the antenna should be less than -10 dB not larger, Figure 3.7.

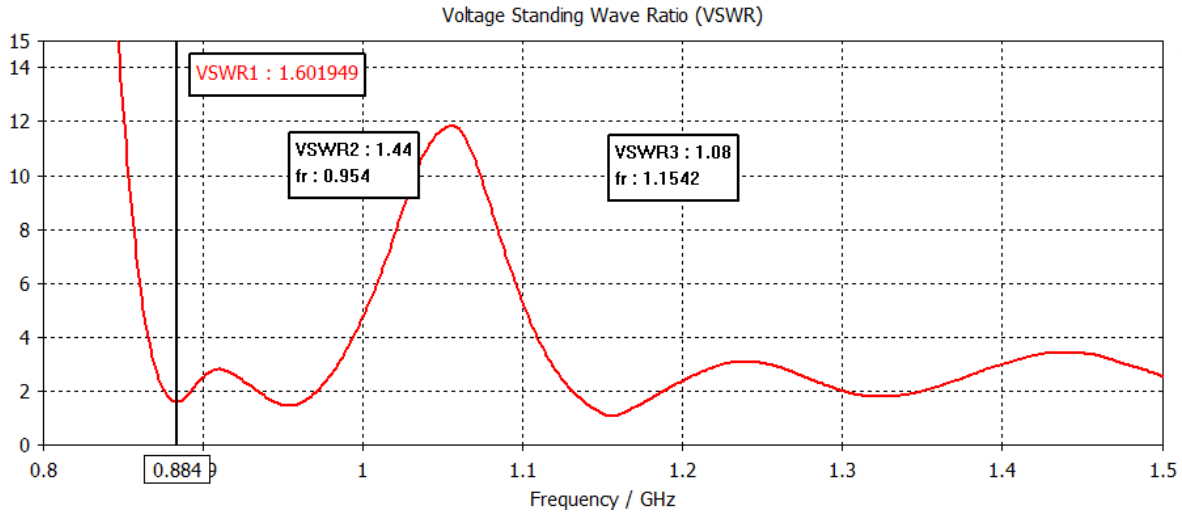

Figure 3.7 VSWR for resonating frequencies for 10x10.5 cm of RSMPA

The far field is another important parameter in antenna design; it can also be visualized at resonating frequencies in the positive z-direction. In addition to the directivities can be shown over phi $\emptyset$ and theta θ angle.

Generally, the plot type of the far field will be a polar at phi $\emptyset$ =0° and 90° in linear scaling mode.

Where $\emptyset = 0°$,

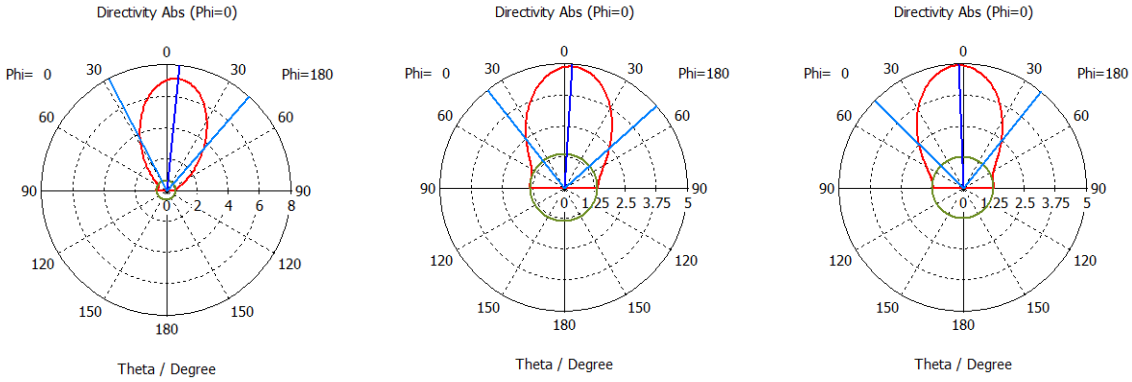

a. $f_0 = 0.884$ GHz b. $f_0 = 0.954$ GHz c. $f_0 = 1.1542$ GHz

Figure 3.8.a Two dimensional normalized far field patterns in linear scaling for 10x10.5 cm of RSMPA at $\emptyset = 0°$

and at $\emptyset = 90°$,

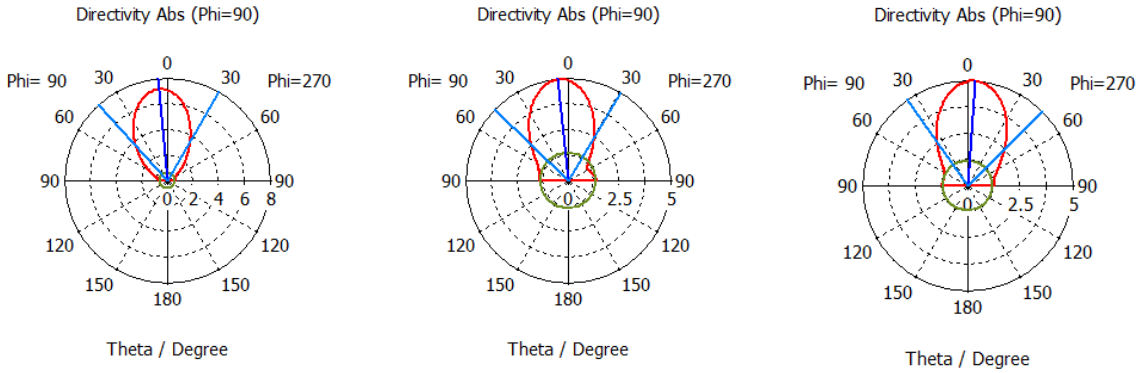

a. $f_0 = 0.884$ GHz b. $f_0 = 0.954$ GHz c. $f_0 = 1.1542$ GHz

Figure 3.8.b Two dimensional normalized far field patterns in linear scaling for 10x10.5 cm of RSMPA at $\emptyset = 90°$

All three patterns yield the different angular separation between two identical points on opposite side to define half power beamwidth HPBW.

The following screenshots show the three dimensional radiation patterns determined in the far field region and represented in z-direction, the directivities are over the angles theta θ and phi $\emptyset$, they also have a good values at resonated frequencies shown in the Table 3.2.

The location and physical dimensions of the probe of the rectangular spiral shaped microstrip patch antenna (RSMPA) had been taken into account to optimize input resistance of 50.96 Ω.

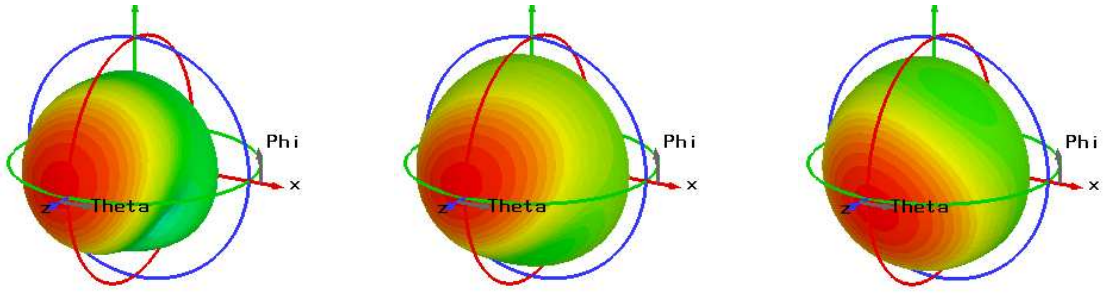

a. $f_0 = 0.884$ GHz b. $f_0 = 0.954$ GHz c. $f_0 = 1.1542$ GHz

Figure 3.9 Three dimensional far field patterns for 10x10.5 cm of RSMPA

Table 3.2 Summary of simulated results in fifth case of RSMPA with reflector

No	f_0 (GHz)	S-Parameters (dB)	Directivity (dBi)	VSWR	HPBW		Side lobe level (dB)
					$\emptyset = 0°$	$\emptyset = 90°$	
1.	0.884	-12.731	8.582	1.6	34.7°	36.05°	-10.4
2.	0.954	-14.774	6.955	1.44	43.3°	38.2°	-5.6
3.	1.1542	-27.316	6.978	1.08	42.2°	39.95°	-6.2

According to the equation 2.2 and its condition into chapter 2, all results of directivities “D” in the summery Table 3.2 are actual values.

The results obtained at the fifth case have gotten better than cases that preceded it. There are many experiments could have done to get new results, but I stopped at the fifth case which achieved the aim of the antenna design.

3.2.10 Analysis of Theoretical Results of RSMPA for 10x10.5 cm

When some analysis and comparisons between the previous cases done. We will clearly see and notice the increasing regularly into the number of angular coils which dependent on rectangular patch, will be the reason of reducing frequency, narrow beam, and the size is acceptable as a small size. As well as the directivities, HPBW and VSWR have good results. With notation in all cases above, the conditions of substrate height with its dielectric constant value and feeding probe were identical and similar.

Even with, the different in the formulation's results, the output of formulation (3.1e) and (3.6a) are the nearest values to the investigated s-parameter curve as shown in Figure 3.6. But in the fifth case the side lobes take a worse assessment.

Ideally, the chart bellow illustrates the resonated frequencies in all cases and could notice that the fifth case was the accepted and better case, which their resonant frequencies between 0.884 GHz and 1.15 GHz. The lower columns represented the fifth case, which is the optimum case.

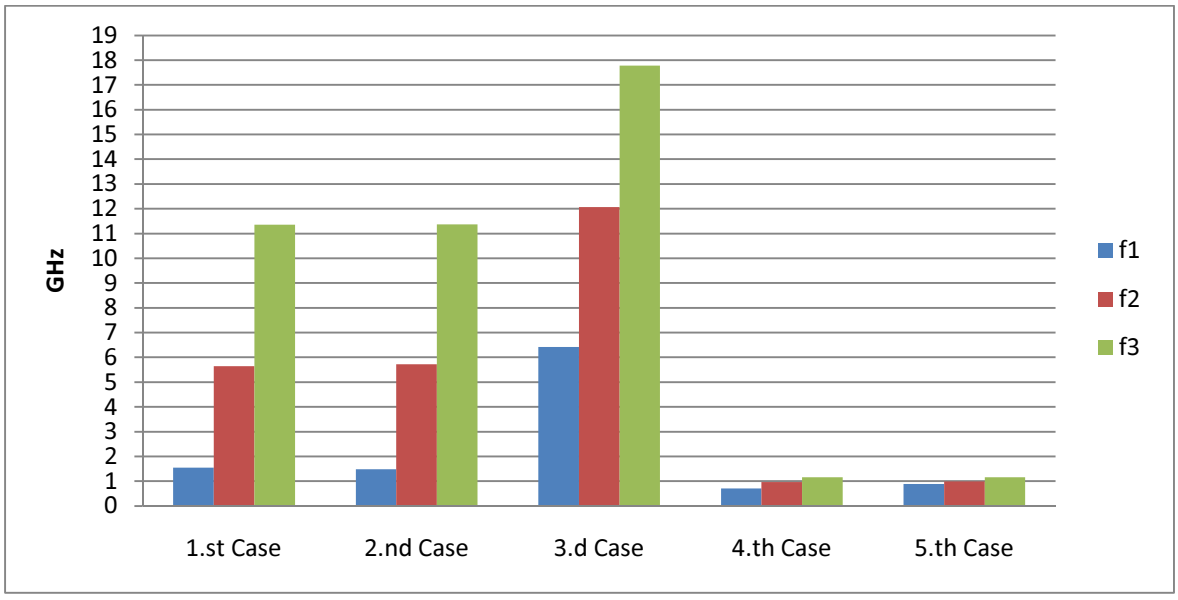

Figure 3.10 Chart of resonated frequencies in all cases

For the similarities in the numeric values in the fourth and fifth cases, makes them appearing in the same level as shown on the Figure 3.10, but the fifth case has the good and required results.

3.3 THE SECOND ANTENNA: RECTANGULAR SPIRAL SHAPED MICROSTRIP PATCH 3.5x3.7 CM

3.3.1 Substrate Selection

In the second type of patch antenna, the selected substrate material is Rogers RT 5880 (lossy) with dielectric constant $\varepsilon_r = 2.2$, height h = 0.1588 cm, and the tangent loss δ is 0.0009. The width of substrate $W_s = 3.5$ cm and the length $L_s = 3.7$ cm.

3.3.2 Width and Length of RSMPA 3.5x3.7 cm

In this design the width W will be reduces to 3 cm and the length L also reduced to 3.2 cm from the previous larger antenna simulation. With the notation, the selected width W had selected carefully to keep the input resistance in the range of 48 Ω to 60Ω.

As aforementioned in the previous larger antenna design 10x10.5cm, the same procedure has been used in the second antenna design, with taken into account the new smallest dimensions.

I do not have to do the same formulation analysis that was done previously, so here I will report the all cases without formulation design procedure. However, the design, simulation, analysis and comparison shall be detailed. The input impedance will only be calculated and compared as shown in the final case below.

3.3.3 First Case

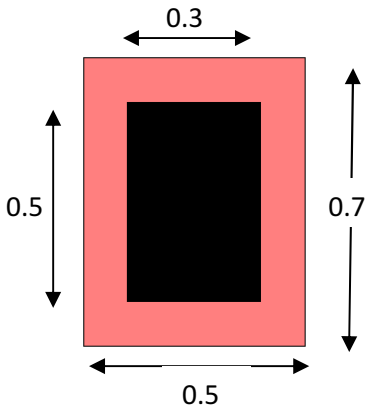

Figure 3.11 Experimental model of mid part of rectangular patch antenna

Simulated Figure 3.11 outputted resonant frequencies at 2.5287 GHz, and 13.927 GHz, which the desired other results were worse. This let me to improve the performance of the antenna as will be done in the cases bellow (See Appendix A).

3.3.4 Second Case

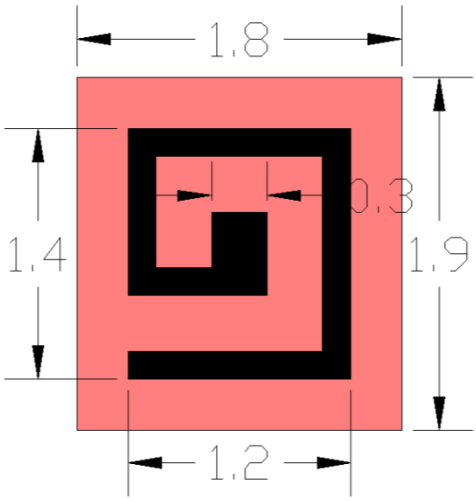

Figure 3.12 Experimental model of rectangular patch antenna with one angular coil

Table 3.3 Summary of simulated results in second case of smaller RSMPA

No	f_0 (GHz)	S-Parameters (dB)	Directivity (dBi)	VSWR	HPBW
1.	2.767	-16.852	worse	1.59	worse
2.	4.853	-17.111	7.094	1.324	43.65°
3.	6.715	-12.843	6.957	1.112	39.35°

The summary Table 3.3 shows the simulated results at resonated frequencies, where phi (∅) =90°, there is a main lobe direction value of 2° at f_0=6.715 GHz.

According to the equation (2.2) and its condition into chapter 2, all shown results of directivities "D" in the summery Table 3.3 are actual values (See Appendix A).

3.3.5 Third Case

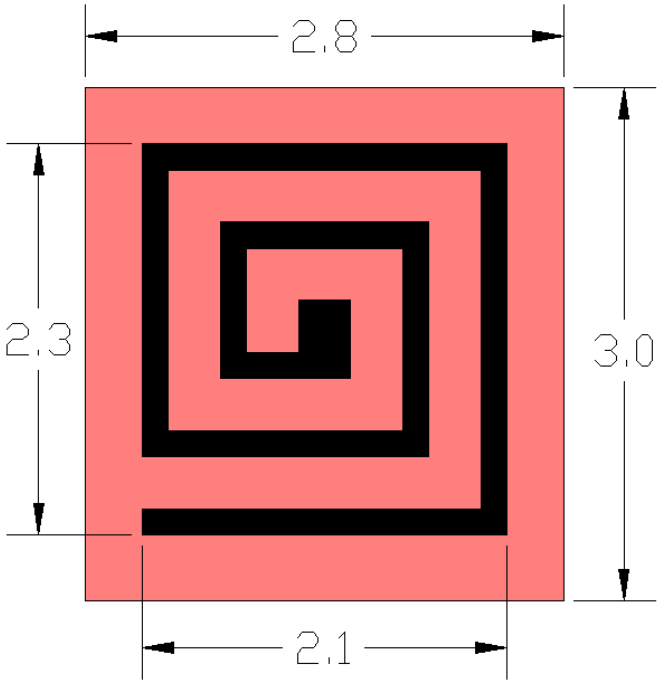

Figure 3.13 Experimental model of rectangular patch antenna with two angular coils

In this case, the resonated frequencies have well results when $f_\circ = 2.1213$ and 2.892 GHz , but at $f_\circ = 1.265$ GHz has a worse result (See Appendix A).

Table 3.4 Summary of simulated results in third case of smaller RSMPA

No	f_0 (GHz)	S-Parameters (dB)	Directivity (dBi)	VSWR	HPBW $\emptyset = 90°$
1.	1.2658	-7.887	worse	worse	worse
2.	2.1213	-17.111	5.477	1.324	63.1°
3.	2.8927	-25.451	7.026	1.112	44.1°

According to the equation 2.2 and its condition into chapter 2, all shown results of directivities “D” in the summery Table 3.4 are actual values.

3.3.6 Fourth Case

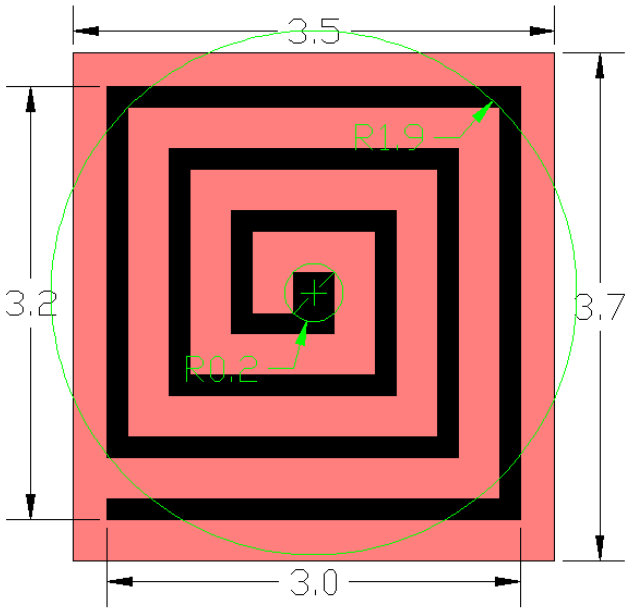

Figure 3.14 Experimental model of rectangular patch antenna with three angular coils

The simulation of the model in Figure 3.14 is the final of rectangular spiral shaped microstrip patch antenna (RSMPA), the results have outputted the good result compared with the model in the previous cases. In addition to achieve the desired aims of the design, low frequency, small size *W*= 3.5 cm and *L* = 3.7 cm, and narrow beam.

With substituting the values of inner and outer radiuses ($r_{inner} = 0.2$ cm, $r_{outer} =$ 1.9 cm) into the equation (3.6) and (3.7) respectively, the output of $f_{low} = 2.5$ GHz and $f_{high} = 23.87$ GHz. From these results we find just the f_{low} is very close to obtained resonant frequency in the simulation.

3.3.7 Characteristic Impedance

Under the condition, $W_0/h \leq 1$, Z_0 may be calculated by:

Firstly, ε_{reff} from equation (3.2)

$$\varepsilon_{reff} = \frac{2.2+1}{2} + \frac{2.2-1}{2}\left[1 + 12\frac{0.1588}{3}\right]^{-1/2} = 2.06 \qquad (3.2b)$$

Secondly, substitute (3.2b) and both of width of microstrip line W_0= 0.15 cm and height of substrate h = 0.1588 cm of values into equation (3.8)

$$Z_0 = \frac{60}{\sqrt{2.06}} ln\left[\frac{8x0.1588}{0.15} + \frac{0.15}{4x0.1588}\right] = 90.46\ \Omega \qquad (3.8b)$$

This Z_0 formula can effectively match characteristic impedance of the patch antenna as shown in (3.8b), however the simulated value of Z_0 yields to 52.9 Ω approximately. It was being by adjusting the outer and inner cylinder radiuses of feeding probe, to be the radius of inner cylinder is 0.08 cm and the radius of outer cylinder is 0.265 cm. The obtained value in (3.8b) is very high compared with simulated.

After the rectangular antenna (RSMPA) model simulated using the final shape shown Figure 3.14. The following item displays the results and analysis of the design.

3.3.8 Results

It shows from Figure 3.15 the resonating frequencies are multiple 1.6188 GHZ, 2.043 GHz, and 2.454 GHz dependent on return losses -11.161 dB, -16.652 dB, and -28.377 dB respectively, and also its -10 dB bandwidths are 0.05675 GHz, 0.10533 GHz, and 0.14513 GHz.

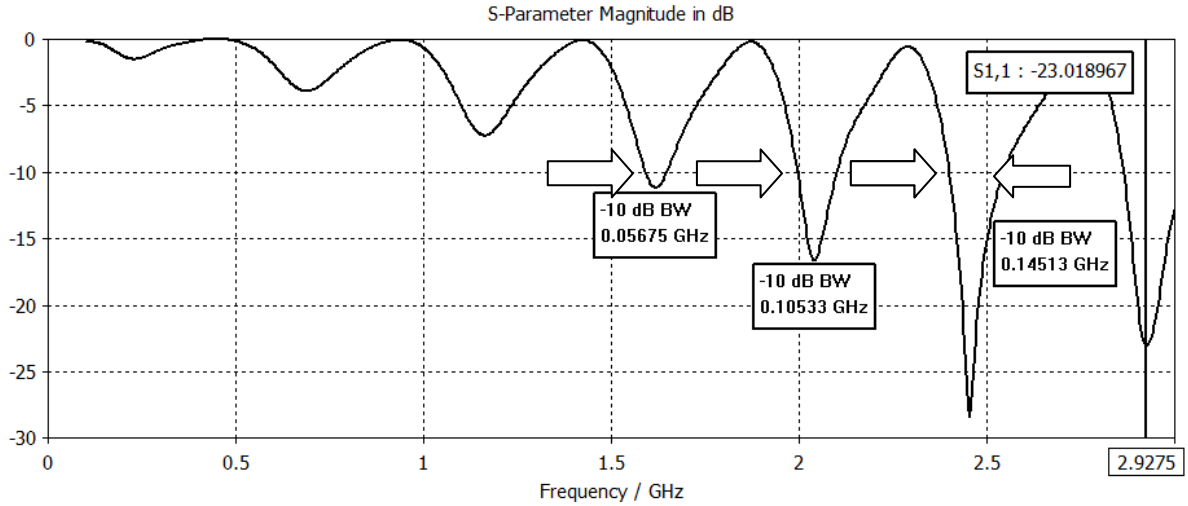

Figure 3.15 S-Parameters for resonating frequencies for 3.5x3.7 cm of RSMPA

The used bandwidth is -10 dB and/or less, to be the reason of improving the VSWR values as shown in Figure 3.16.

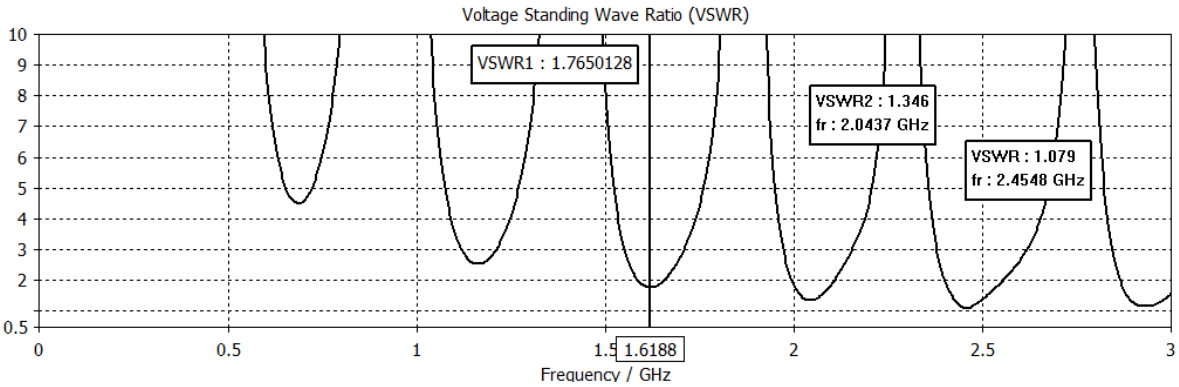

Figure 3.16 VSWR for resonating frequencies for 3.5x3.7 cm of RSMPA

The far field amplitude patterns directed in positive z and visualized over phi $\emptyset$ and theta θ angles as can be shown in the following Figure 3.17. While the plot is two dimensional in linear scaling at phi $\emptyset$ =0° and 90°.

Where $\emptyset = 0°$,

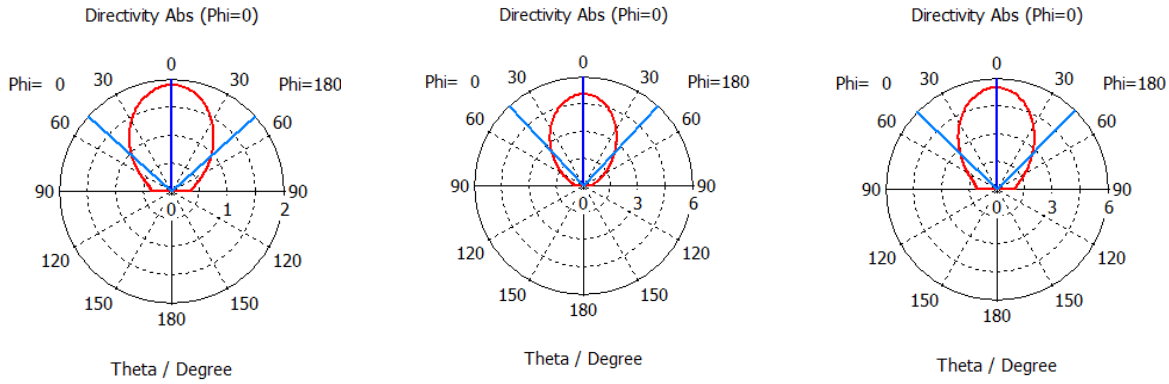

a. $f_0 = 1.6188\ \text{GHz}$ b. $f_0 = 2.0437\ \text{GHz}$ c. $f_0 = 2.4548\ \text{GHz}$

Figure 3.17.a Two dimensional normalized far field patterns in linear scaling for 3.5x3.7 cm of RSMPA at $\emptyset$ =0°

and at $\emptyset = 90°$,

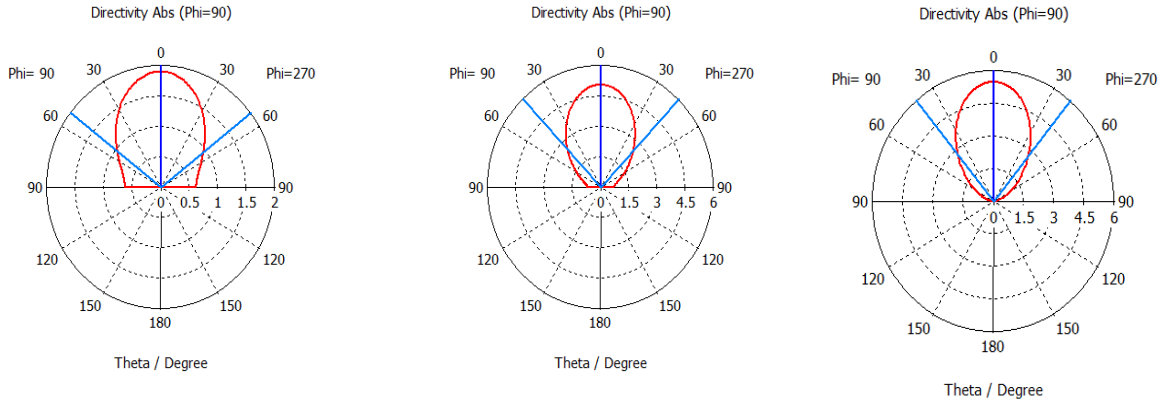

a. $f_0 = 1.6188\ \text{GHz}$ b. $f_0 = 2.0437\ \text{GHz}$ c. $f_0 = 2.4548\ \text{GHz}$

Figure 3.17.b Two dimensional normalized far field patterns in linear scaling for 3.5x3.7 cm of RSMPA at $\emptyset$ =90°

From Figure 3.17 is clearly half power beamwidth HPBW shown that all angles are smaller and acceptable.

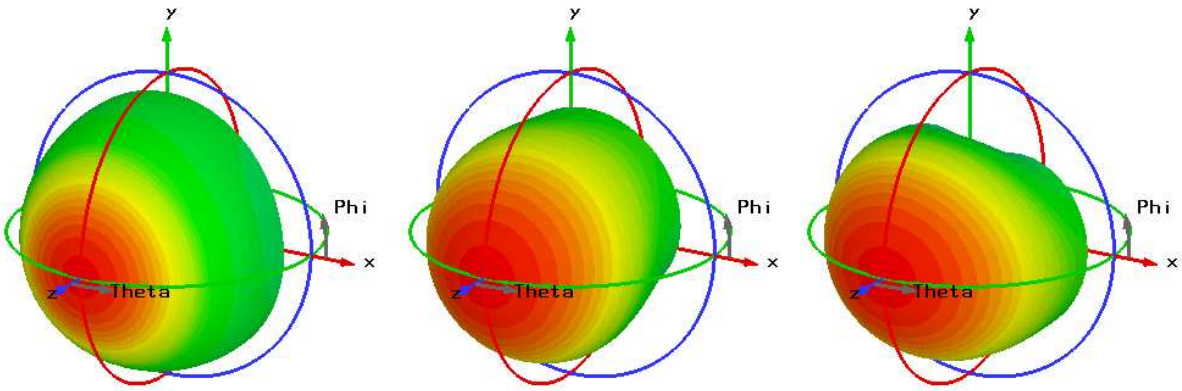

a. $f_0 = 1.6188\ \text{GHz}$ b. $f_0 = 2.0437\ \text{GHz}$ c. $f_0 = 2.4548\ \text{GHz}$

Figure 3.18 Three dimensional far field patterns for 3.5x3.7 cm of RSMPA

No worse results observed in the simulation of the final case as shown in the summarized Table 3.5.

Table 3.5 Summary of simulated results in fourth case of smaller RSMPA

No	f_0 (GHz)	S-Parameters (dB)	Directivity (dBi)	VSWR	HPBW	
					Ø =0°	Ø =90°
1.	1.6188	-11.161	2.758	1.765	48°	52.5°
2.	2.043	-16.652	7.012	1.346	42.9°	43.6°
3.	2.454	-28.377	7.381	1.079	45.1°	39.5°

Based on the reference value of equation (2.2) into chapter 2, the gotten outputs of directivities "D" in summery Table 3.5 are actual values. That means the conditions dependent on λ were truly investigated.

3.3.9 Analysis of Theoretical Results of RSMPA for 3.5x3.7 cm

From the show results of follow up cases, the of final case is the optimum in obtained outputs which demonstrate, the aim of design antenna, which can be summarized in small size, narrow bean, and low frequency.

In the third case some good and accepted results were gotten as shown in Table 3.4. However, the results entirely acceptable were in the final case that maintains the objective of the antenna design.

In view of the evaluating both of $f_{low}\ and\ f_{high}$ by the equations (3.6) and (3.7) the gotten result of $f_{low} = 2.5$ GHz is very close to simulated and shown in the last row in Table 3.5.

While the distance between angular coils increasing constantly, the size of the shape of RSMPA also increases the width *W* and the length *L* that affected the results positively.

The chart bellow illustrates the change of resonant frequencies, it also indicates, whenever moving from a case to the next the value of resonant frequency improves.

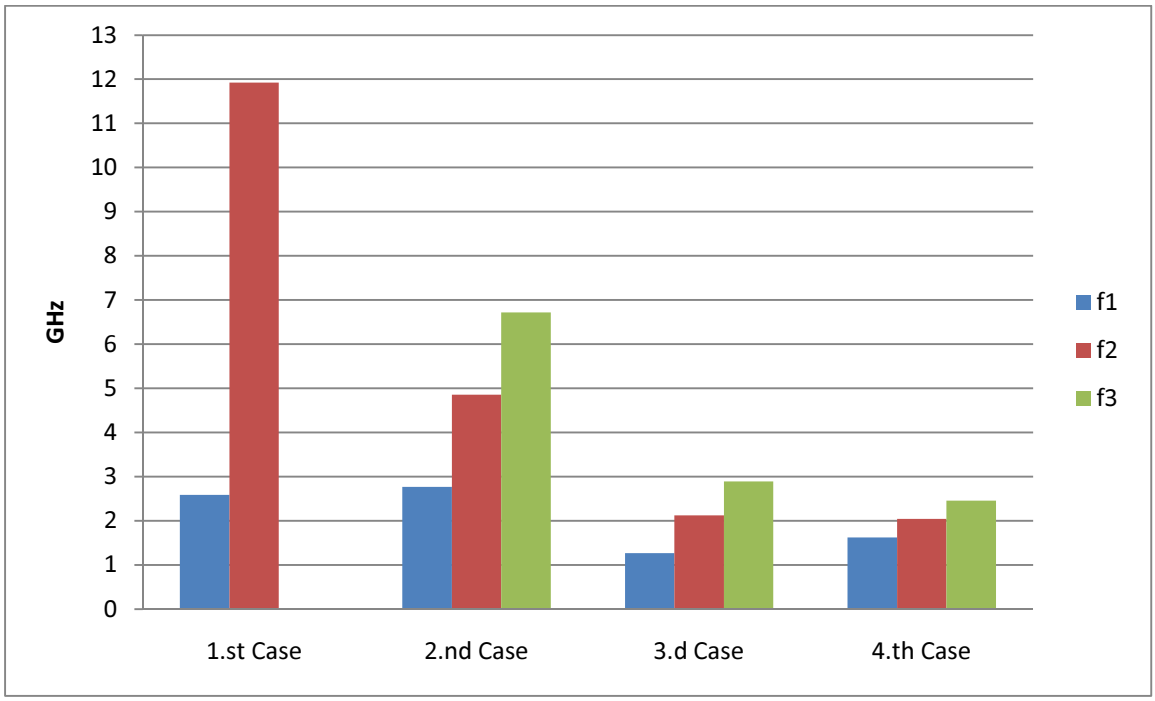

Figure 3.19 Chart of resonated frequencies of smaller RSMPA

3.4 THE THIRD ANTENNA: CIRCULAR SPIRAL SHAPED MICROSTRIP ANTENNA (CSMPA) 2.8x2.8 CM

3.4.1 Sustrate Selection

In the third and final type of patch antennas, the substrate form will be rectangular, the selected material is Rogers RT 5880 (lossy) with dielectric constant $\varepsilon_r = 2.2$, height *h* = 0.1588 cm, and the tangent loss δ is 0.0009. The properties of substrate in the third case

same with the second case. However, the different is in the sizes of width $W_s = 2.8$ cm and length $L_s = 2.8$ cm of substrate.

3.4.2 Radius of Patch

In this design the radius *a* of patch located in the center, has 0.15 cm radius as shown in the first case of design Figure 3.20, with added arms in every case, it consists of many radiuses for each case or adding coil as shown in Figures 20, 21,and 22, in reference to previous, in adding each circular coil the new radius will be consisted of and the general size of the metallization will grow spaced with empty areas between circular coils.

As aforementioned in the previous larger antenna designs (RSMPA) 10x10.5cm and 3.5x3.7cm, the same procedure has been used in the final antenna design, with taken into account the new smallest dimensions and differences. The formulations will be applied to see the different between the chosen and gotten size of radius. The optimum size of substrate and radiuses will be utilized.

3.4.3 First Case

In the first case the basic circular microstrip patch antenna is represented with radius *a* = 0.15 cm, and this is the first assuming to obtain the aim of the thesis in the second type of antennas.

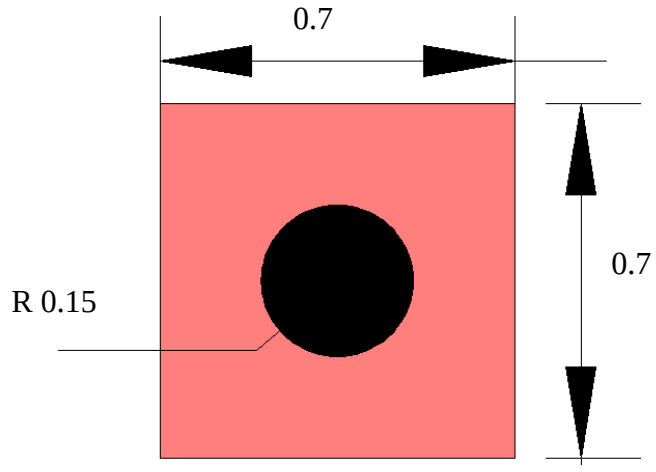

Figure 3.20 Experimental model of circular patch antenna

By the following formula, the resonant frequency may be calculated

$$f_0 = \frac{1.8412\ c}{2\pi a\sqrt{\varepsilon_r}} \tag{3.9}$$

Where c is the speed of light in free-space, and *a* is the radius of patch.

$$f_0 = \frac{1.8412 * 30}{2\pi 0.15\sqrt{\varepsilon_r}} = \ 39.51\ \text{GHz} \tag{3.9a}$$

Indeed, the obtained result in equation (3.9a) was much larger than required. So the sequence in cases will continue (See Appendix A).

3.4.4 Second Case

In the second case, the first experiment will be by adding circular coil which starts from radius $r_{11} = 0.15$ cm and ends at $r_{12} = 0.4$ cm with rotation of 360°, as it is shown in Figure 3.21 the first circular coil does not start from the center, but 0.15 cm distance away, and unites with the circular patch located at the center, with notation that the coil is not a closed circle, it circles identically and smoothly from point to end at another.

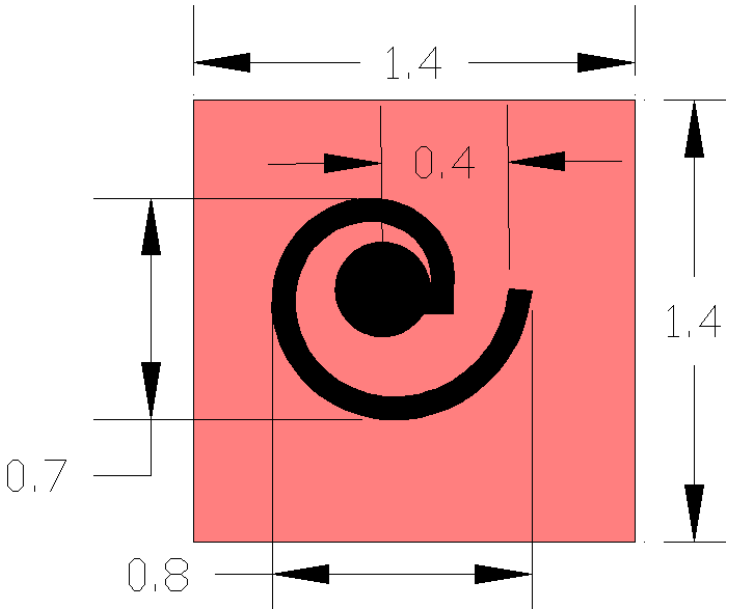

Figure 3.21 Experimental model of circular patch antenna with one circular coil

The Figure 3.21 has combined between the patch and spiral; therefore, the evaluated frequencies will be dependent upon Archimedean spiral formulations.

The low frequency operating point of the spiral is determined theoretically by the outer radius r_2 and is given by

$$f_{low} = \frac{c}{2\pi r_2} \tag{3.6}$$

Where c is the speed of light.

$$r_2 = r_{12} + \frac{W_a}{2} \tag{3.10}$$

Where $W_a = 0.075$ cm is considered the width of the arm, and $r_2$is the radius from the center to the end edge of first coil $r_{12} = 0.4$ cm plus the width W_a divided to two.

$$r_2 = 0.4 + \frac{0.075}{2} = 0.4375 \text{ cm} \tag{3.10a}$$

By substituting the values depicted above into equation (3.6)

$$f_{low} = \frac{30 * 10^9}{2\pi\ 0.4375} = 10.9 \text{ GHz} \tag{3.6b}$$

Similarly the high frequency operating point is based on the inner radius giving

$$f_{high} = \frac{c}{2\pi r_1} \tag{3.7}$$

$$r_1 = r_{11} + \frac{W_a}{2} \tag{3.11}$$

Where $r_1$is the radius from the center to the first point of first coil plus the width W_a divided to two.

$$r_1 = 0.15 + \frac{0.075}{2} = 0.1875 \text{ cm} \tag{3.11a}$$

By substituting the values depicted above into equation (3.7)

$$f_{high} = \frac{30 * 10^9}{2\pi\ 0.1875} = 25.5 \text{ GHz} \tag{3.7b}$$

The spotted values in the second case, additionally to the value of f_0 obtained in the first case; the frequencies are too higher than required. The simulation also exhibits the resonant frequencies in multi points and at high values, which make us think and report that the differences in values shown from combining the parameters of two antennas to each other (See Appendix A).

3.4.5 Third Case

Thus, from calculated and simulated results in the second case that prompted me to reconfigure the patch by adding second circular coil under same conditions explained previously.

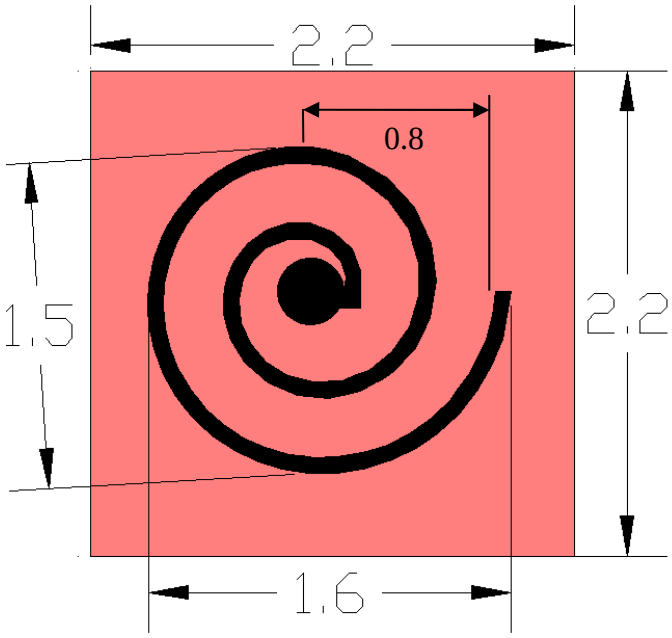

Figure 3.22 Experimental model of circular patch antenna with two circular coils

The low frequency operating point of the spiral is determined theoretically by the outer radius r_3 and is given by

$$f_{low} = \frac{c}{2\pi r_3} \tag{3.6}$$

$$r_3 = r_{13} + \frac{W_a}{2} \tag{3.12}$$

Where $W_a = 0.075$ cm is considered the width of the arm, and $r_3$is the radius from the center to the end edge of second coil $r_{13} = 0.8$ cm plus the width W_a divided to two.

$$r_3 = 0.8 + \frac{0.075}{2} = 0.8375 \text{ cm} \tag{3.12a}$$

By substituting the values depicted above (3.12a) into equation (3.6)

$$f_{low} = \frac{30}{2\pi\ 0.8375} = 5.7 \text{ GHz} \tag{3.6c}$$

In view of the results above, the f_{low} value is reduced approximately 50 % for the second case. The reason is in increasing the metallization part of patch by adding the second circular coil onto the patch. But, f_{high} always has a constant value in all case.

The simulation is resulted approximate resonated frequency at $f_0 = 4.951$ GHz, while the calculated $f_{low} = 5.7$ GHz , the simulation has values of 2.2483 GHz, 3.664 GHz, and 4.951 GHz (See Appendix A).

Table 3.6 Summary of simulated results in second case of CSMPA

No	f_0 (GHz)	S-Parameters (dB)	Directivity (dBi)	VSWR	HPBW Ø =90°
1.	2.2483	-10.941	worse	1.792	worse
2.	3.664	-27.845	7.012	1.0844	47.8°
3.	4.951	-15.905	7.381	1.3815	40.95°

3.4.6 Fourth Case

This is the final case which formed as a new shape of required, by adding the third circular coil as shown in the Figure 3.23.

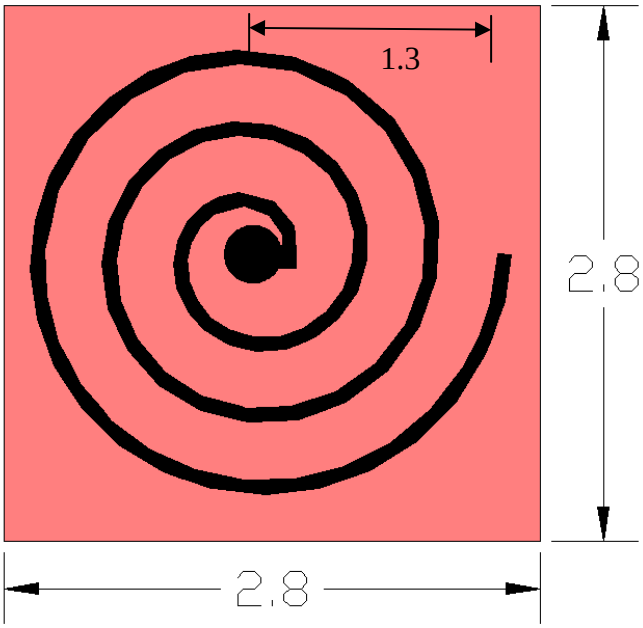

Figure 3.23 Experimental model of circular patch antenna with three circular coils

The low frequency operating point of the spiral is determined theoretically by the outer radius r_4 and is given by

$$f_{low} = \frac{c}{2\pi r_4} \tag{3.6}$$

$$r_4 = r_{14} + \frac{W_a}{2} \tag{3.13}$$

Where $W_a = 0.075$ cm is considered the width of the arm, and $r_3$is the radius from the center to the end edge of second coil $r_{14} = 1.3$ cm plus the width W_a divided to two.

$$r_4 = 1.3 + \frac{0.075}{2} = 1.3375 \text{ cm} \tag{3.13a}$$

By substituting the values depicted above (3.12a) into equation (3.6)

$$f_{low} = \frac{30}{2\pi\ 1.3375} = 3.569 \text{ GHz} \tag{3.6d}$$

As shown in equation (3.6d) $f_{low} = 3.569$ GHz, is a result that located between simulated results which the simulation has resonated frequencies at 2.6443 GHz, 3.3076 GHz, 3.9808 GHz, and 4.7431 GHz.

This is the optimum form and values which achieved the aim of the thesis as shown by figures, summarized table, and analysis in the result part.

3.4.7 Characteristic Impedance

The obtained characteristic impedance of simulation (CSMPA) is 50.38 Ω. The same ways have been used here to got a good value of Z_0, that represented by controlling the radius of inner cylinder which consists of PEC and outer cylinder which consists of substrate's material of Rogers RT5880.

3.4.8 Results

From Figure 3.24 the resonating frequencies are multiple 2.644 GHz, 3.3076 GHz, 3.9808 GHz, and 4.7431 GHz dependent on return losses -13.89 dB, -23.206 dB, -24.493 dB, and -16.181 dB respectively, and also its -10 dB bandwidths are 0.098022 GHz, 0.13495 GHz, 0.15751 GHz, and 0.13827 GHz.

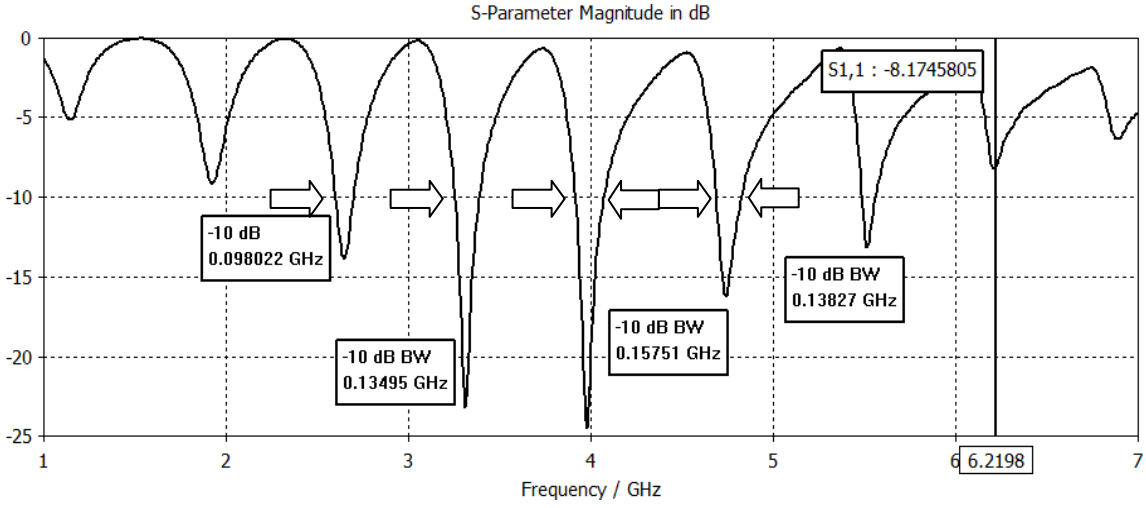

Figure 3.24 S-Parameters for resonating frequencies for 2.8x2.8 cm of CSMPA

The shown values of VSWR are in the range from 1 to 2 that means good results of VSWR were investigated by the simulation.

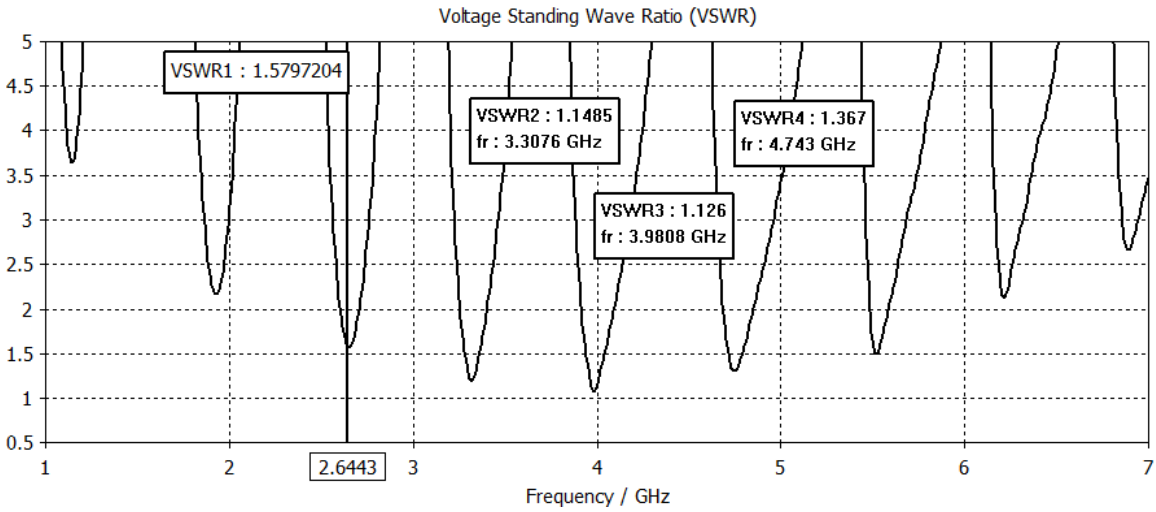

Figure 3.25 VSWR for resonating frequencies for 2.8x2.8 cm of CSMPA

We now present a few results for the radiation patterns; the far field is visualized at resonating frequencies in the positive z-direction. In addition to the directivities can be shown over phi $\emptyset$ and theta θ angle.

Generally, the plot type of the far field will be a polar at phi ∅ =0° and 90° in linear scaling mode.

Where ∅ =0°,

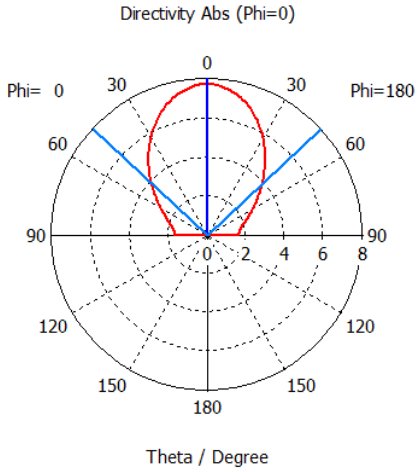

a. $f_0 = 2.6443$ GHz

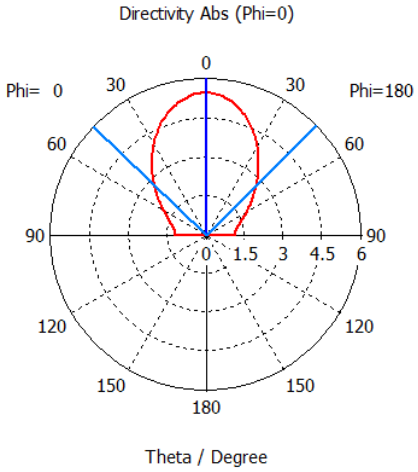

b. $f_0 = 3.3076$ GHz

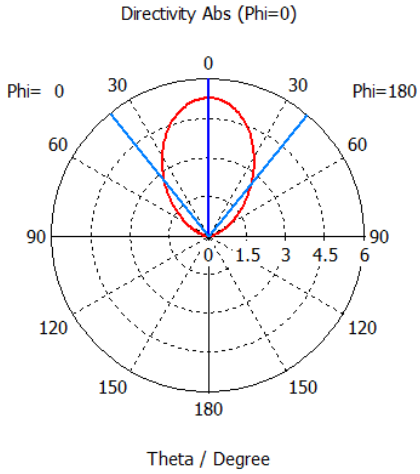

c. $f_0 = 3.9808$ GHz

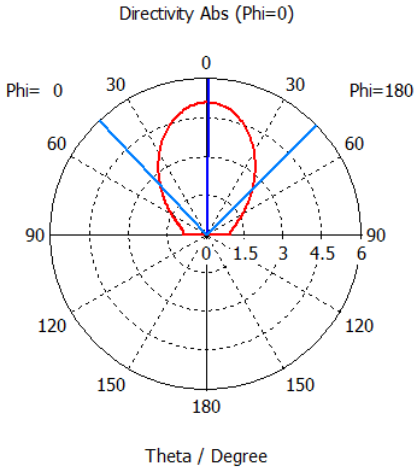

d. $f_0 = 4.7431$ GHz

Figure 3.26.a Two dimensional normalized far field patterns in linear scaling for 2.8x2.8 cm of RSMPA at ∅ =0°

and at Ø =90°,

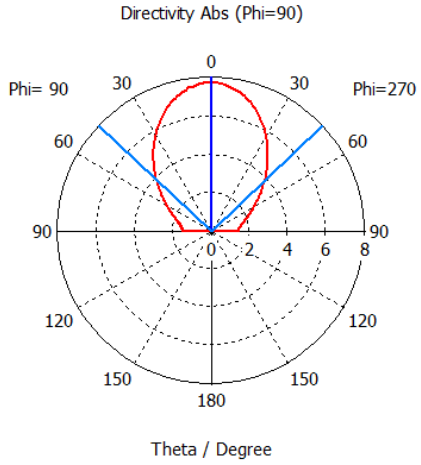

a. $f_0 = 2.6443$ GHz

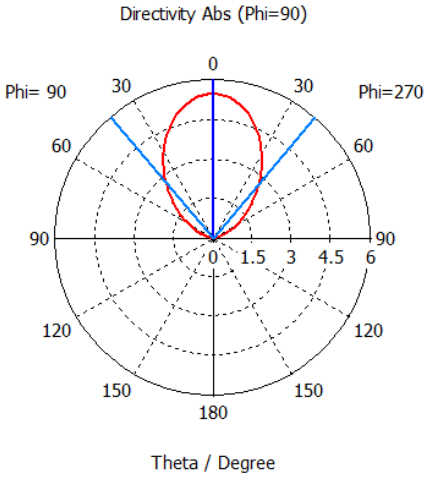

b. $f_0 = 3.3076$ GHz

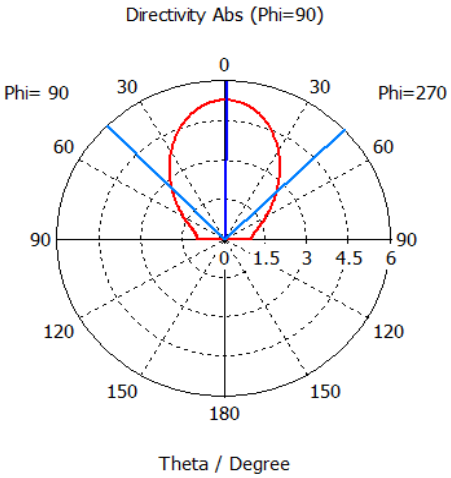

c. $f_0 = 3.9808$ GHz

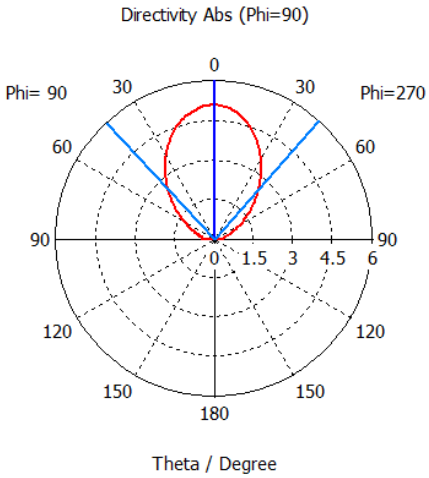

d. $f_0 = 4.7431$ GHz

Figure 3.26.b Two dimensional normalized far field patterns in linear scaling for 2.8x2.8 cm of CSMPA at Ø =90°

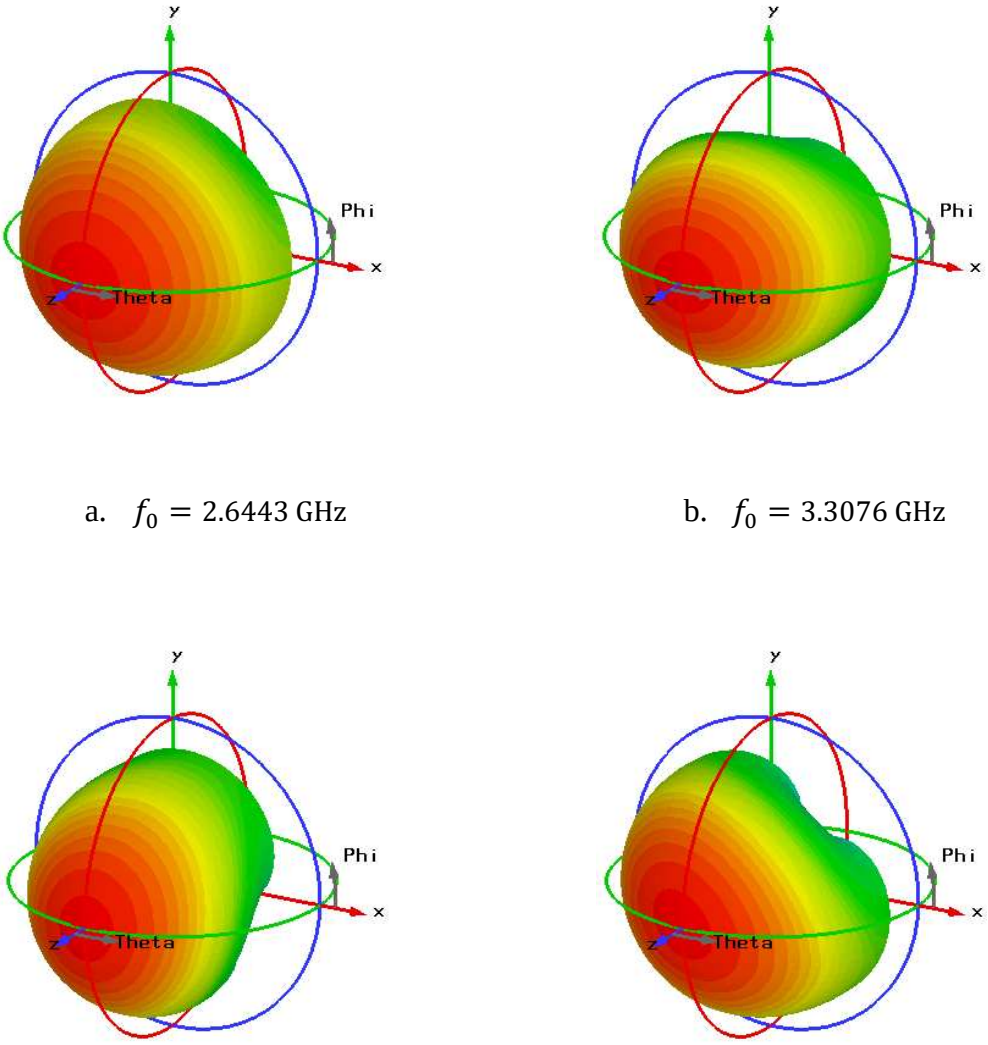

a. $f_0 = 2.6443$ GHz

b. $f_0 = 3.3076$ GHz

c. $f_0 = 3.9808$ GHz

d. $f_0 = 4.7431$ GHz

Figure 3.27 Three dimensional far field patterns for 2.8x2.8 cm of CSMPA

Table 3.7 Summary of simulated results in fourth case of CSMPA

No	f_0 (GHz)	S-Parameters (dB)	Directivity (dBi)	VSWR	HPBW	
					$\emptyset = 0°$	$\emptyset = 90°$
1.	2.6443	-13.890	8.885	1.506	47.25°	46.65°
2.	3.3076	-23.206	7.373	1.148	45.8°	40.15°
3.	3.9803	-24.493	7.231	1.126	39.1°	45.3°
4.	4.7431	-16.181	7.063	1.367	44.3°	42.25°

According to the equation 2.2 and its condition into chapter 2, all shown results of directivities “D “ in the summery Table 3.7 are actual values.

3.4.9 Analysis of Theoretical Results of CSMPA for 2.8x2.8 cm

From tracking cases of design circular spiral microstrip patch antenna (CSMPA), the final case was the better than previous. With notation, in the third type of antennas the spiral formulations was applied to discover the range of frequency was highest then decreased steeply as shown in the final case. In comparison with patch frequency evaluation equations the results were convergent.

In the first case, the applied formula was a circular patch formula which depends on a radius of circle,in addition to frequency is resonated at one point 4.04 GHz, but in the next cases, the used formulas were spiral formulas which f_{low} has approximately same value of simulated and the frequency was resonated at multiple points.

The following chart presents the value of resonated frequency in the first case was one, and in the progress of cases became multiple.

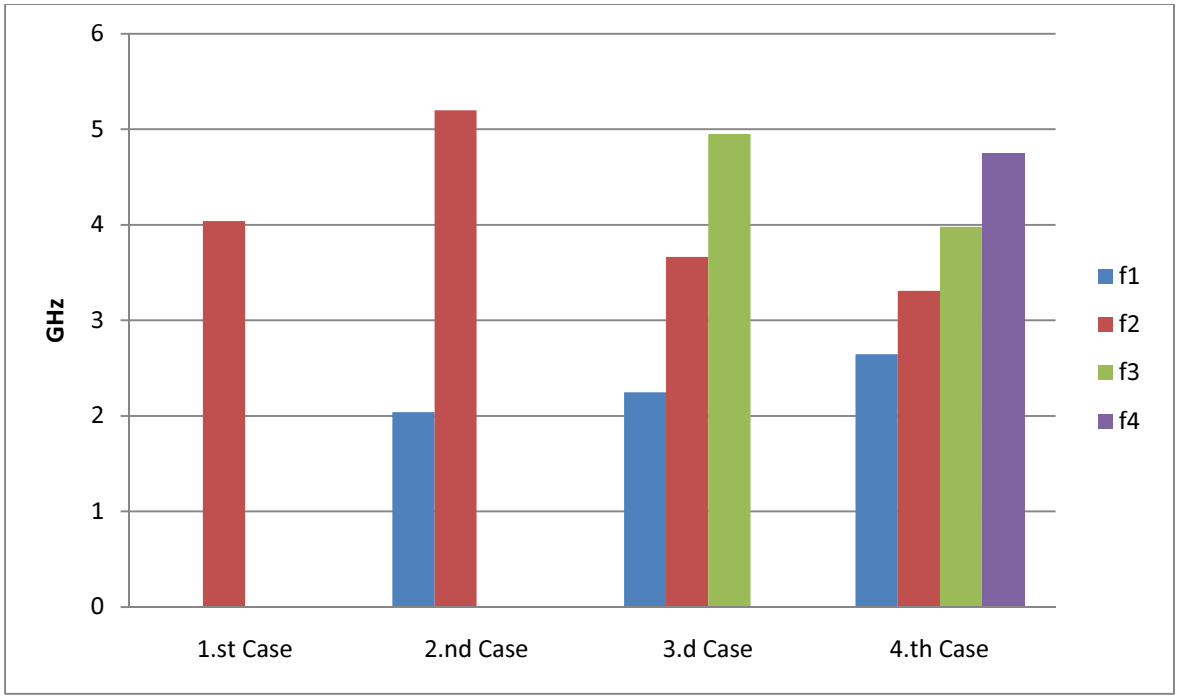

Figure 3.28 Chart of resonated frequencies in all cases of CSMPA

3.5 CONCLUSION

The results illustrative in this chapter are numerical, experimental cases of basic characteristic of the rectangular and circular spiral shaped microstrip antennas (RSMSA), (CSMPA). The antennas were studied and analyzed in details to show the effect of various shapes, cases and dimensional parameters on their results, such as 2D and 3D radiation patterns, s-parameters, directivities, gain, bandwidth, and characteristic impedances. For instance, the results showed that in every simulated and calculated case different resonant frequencies had been gotten and some outputs were good others were worse. It also the analysis is done in each case, but the full result was found in the optimum case which was the final case in each simulated antenna. Finally, the chart shows the resonant frequencies in each case.

CHAPTER 4

FABRICAION AND MEASUREMENTS

4.1 INTRODUCTION

For the thesis, I have only constructed two smaller antennas and tested them into micro wave laboratory. The third one I have no find the material of substrate into the local market.

The fabricated and measured antennas were:

1. Rectangular spiral shaped microstrip patch antenna (RSMPA) 3.5x3.7 cm.
2. Circular spiral shaped microstrip patch antenna (CSMPA) 2.8x2.8 cm.

Resonating at multi frequencies, as narrow beam as explained analytically and numerically into theoretical previous chapters and in this chapter of fabrication. In addition, experimental results are often needed to validate theoretical data.

4.2 SIGNIFICANCE OF NARROW BEAM, LOW FREQUENCY AND SMALL SIZES

Since the studies have been started onto researches of the Hyperthermia and GPR, the requests of the parameters of antennas became narrow beam, low frequency and small sizes. The reasons of these demands are more effective, easier to use, could be an array without mentioned damage. It was gotten and clearly shown in the following figures and analysis.

4.3 FABRICATION OF RECTANGULAR SPIRAL SHAPED MICROSTRIP PATCH ANTENNA (RSMPA) 3.5x3.7 CM

4.3.1 Construction of RSMPA 3.5x3.7 cm

1. Front section that metalliztion (PEC) has coiled rectangularly on substrate and shaped spirally.
2. Back section that metallization (PEC) has covered fully the substrate, named ground, drilled in the mid point of radius 0.2 cm as an outer cylinder, but the inner cylinder is about 0.0585 cm to allow access of feeding.
3. Middle section that has a dielectric constant 2.2, called substrate with material of Rogers RT 5880.
4. Female connector that connected between both of the feeding system as a first edge and the port as a second edge.

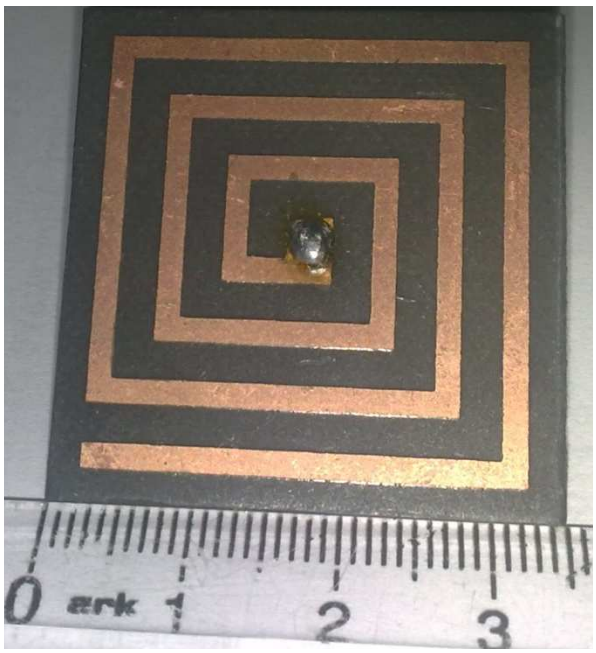

Figure 4.1 Front section of fabricated model of RSMPA 3.5x3.7 cm

4.3.2 Construction of CSMPA 2.8x2.8 cm

As were represented in previous item 1.3.1, the CSMPA has a same form of construction, however the difference is in the size and the shape.

Figure 4.2 Front section of fabricated model of CSMPA 2.8x2.8 cm

4.3.3 Fabrication Steps and Notes

Both antenna designs were fabricated to enable real measurements. Geometry of models had been converted to layout masks and transfered to transparent film, film was used to expose the microstrip lines clearly during the process of photo resistive etching. The challenges we had faced while the exposure and etching are the proper alignments of the turns of the antennas which have multi-turns with specific dimensions of microstrip lines and free area between the turns. The alignment of the multi turns of antennas depend gravely on the convenient placement. And it also has to be adjusted and done with caution.

There was a legitimate danger of damaging or not straight cut of the turns of spiral shaped microstrip lines. After the models were etched and cleaned, manufacturing defect was clearly evident which influenced in the results.

As the last step, SMA connector has been mounted in the center-back of the construction of antenna. That touched and soldered to the microstrip. The important

note here is in SMA connector that being instead of coaxial probe, which has difference features. An SMA connector is used in conjunction with cable television, satellite TV, and any type of internet from cable, to DLS and even fiber optics. But it had to use it so as to be available in the local market.

4.4 INSTRUMENTATION

The instrumentation required to accomplish a measuring task depends largely on the functional requirements of the design.

1. Source antennas (designed and implemented antennas).
2. Positioning system that investigates the far field region without hindrance may weak the transmitted waves or reflect them by unknown angles away.
3. Network analyzer that has mixers, RF source links to the source antenna, and may connect to the computer.
4. Data processing that achieved by the software loaded into the analyzer.

The stability and control of frequency, spectral purity, power level and modulation will be presented by transmitting RF source.

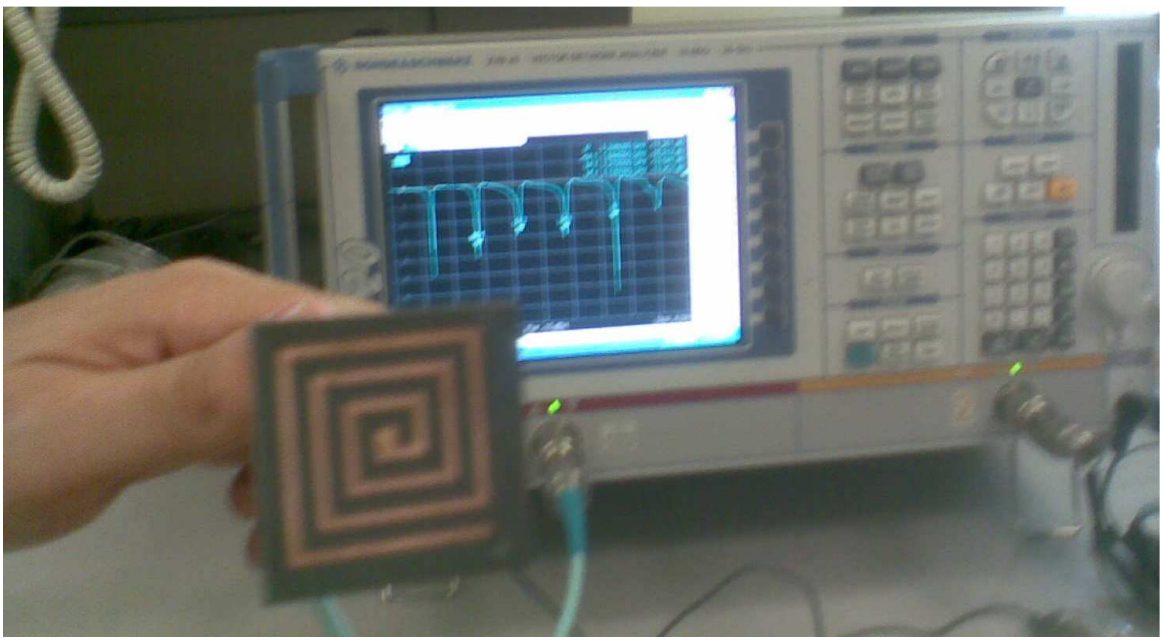

Figure 4.3 Instrumentation for measuring RSMPA 3.5x3.7 cm

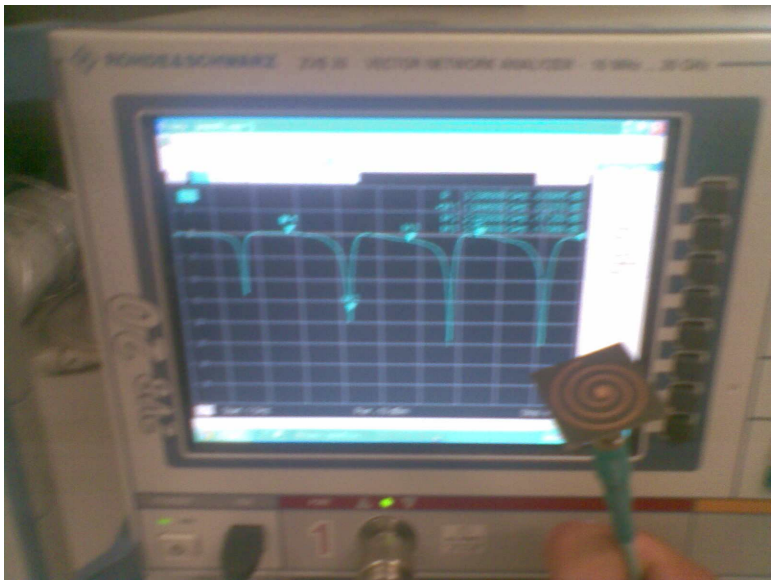

Figure 4.4 Instrumentation for measuring CSMPA 2.8x2.8 cm

As shown from the figures above, the positioning system does not available, the antenna was fixed manually. Therefore, it is the one of many problems faced us in measurement process.

4.5 S-PARAMETER MEASUREMENTS

Measurements were performed by the Rhode&Schwarz ZVB20 Vector Network Analyzer and calibrated to the input of the antenna in 1 GHz – 4 GHz frequency band. Each antenna was measured in the first port setup Figure 4.4. Original measurement values that outputted shown into Figure 4.5 for rectangular spiral shaped microstrip patch antenna, and Figure 4.6 for circular spiral shaped microstrip patch antenna respectively. With overlapping the simulated results in the previous chapter on measured in this chapter.

So the reflections from the antennas at resonated frequency were obtained and plotted in Figure 4.5 and Figure 4.6.

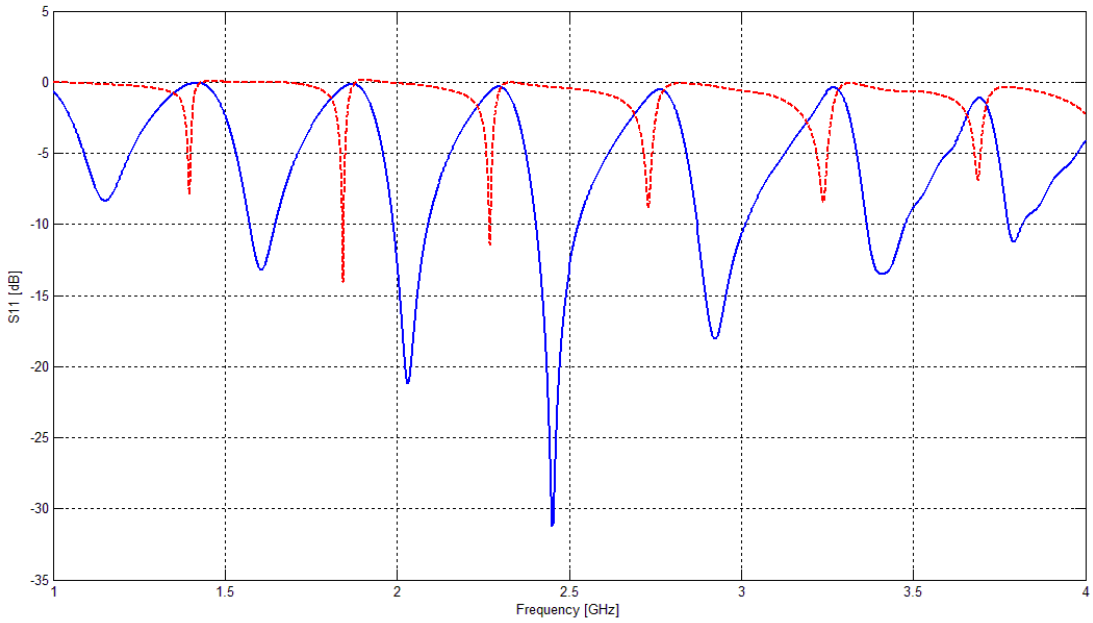

Figure 4.5 S-Parameters for simulated and measured of RSMPA 3.5x3.7 cm

The dotted graphic is the measured, and the non-dotted graphic is the simulated, from the reflections above, we can see the difference in shifting the measured in range of 200 MHz to 250 MHz, which the measured is located in the non-fade period of the simulated.

And also the difference is in the return loss value, since the simulated (Non-dotted) is deepest than the measured (dotted). In addition to dotted graphic is narrower than the non-dotted.

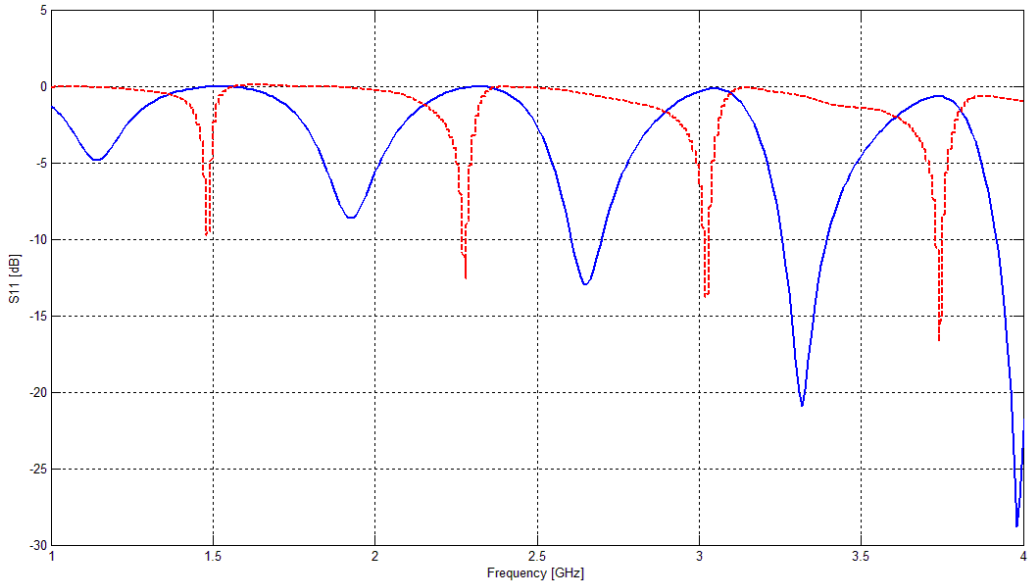

Figure 4.6 S-Parameters for simulated and measured of CSMPA 2.8x2.8 cm

The same note above applies in the second antenna (CSMPA), but the dotted graphic started in deep -10 dB and decreased by -5 dB proximately in each resonated frequency point.

The affected reasons of the obtained results are that shifting and narrower band in the measured, they may be:

The fabrication was not exactly as designed and simulated. The importance other one also is the SMA connector that has not exact properties with coaxial probe. The position of simulated antenna under far region as a condition, but the measured was in the microwave laboratory which includes many electronic instruments and furniture. The final think is that the analyzer may has a different excitation signal, in case the used signal in the simulation was Gaussian signal.

CHAPTER 5

5.1 CONCLUSION

In this study, the various models discussed so far can be grouped into two categories: rectangular and circular models. The categories have separated to three types of reconfigured microstrip patch antennas which were designed, simulated, analyzed and manufactured. The reconfigured patch antenna combined with a spiral to consist of a new form, called spiral shaped microstrip patch antenna (SMPA), which has divided into two parts, the first is a rectangular spiral shaped microstrip patch antenna (RSMPA) includes two forms larger with size 10x10cm and smaller with size 3.5x3.7 cm, the second is a circular spiral shaped microstrip patch antenna (CSMPA) 2.8x2.8 cm. To be reached to the final and optimum case of modeled antennas, it was used the adding method of new angular or circular coils in each case, which leads the results to improvement case. The design and simulation software was CST MICROWAVE STUDIO; the observed results from simulation, mathematical equations and measurements were analyzed, compared, and presented in figures and charts. With a note, that the indicated formulas were the microstrip patch's and spiral's. The feeding systems were coaxial probe in all type of antennas.

From the design, simulation, and measurements the results were convenient to the aim of thesis which focused on small sizes, low frequencies and narrow beam; these properties make the antenna applied especially into the GPR Ground Penetrating Radar and Hyperthermia.

The illustrated results in the final cases of simulations were D directivity, HPBW, Farfield, VSWR, and S-parameters. While the results were computed for rectangular and circular microstrip patch antenna, it also the spiral's formulation had been taken

into account. As well as, the results were valid only for single and isolated microstrip antennas.

5.2 FUTURE PROSPECTS

The microstrip patch antenna has a huge phenomenon over the past and present years. And although much research on designing has been appeared, only it shows there is no located applicable formulation in a new reconfiguration antenna. As a matter of fact, the different between calculated and simulated outputs and the use formulations depends on the approximation; this is a situation that does not give strict and/or net values of results.

Therefore, the future plane will be to derivate applicable formulation for the antennas that have been discussed in this thesis, also to achieve conventional theoretical study.

The keyword may be by the combining between formulas' of microstrip and spiral. As combined in the models.

REFERENCES

[1] National Cancer Institute Fact Sheet 7.3, Hyperthermia in Cancer Treatment: Questions and Answers, 2004. http://www.cancer.gov/cancertopics/factsheet/Therapy/hyperthermia.

[2] Chou, Chung-Kwang, “Application of Electromagnetic Energy in Cancer Treatment”, IEEE Transactions on Instrumentation and Measurement, Vol. 31, No. 4. December 1988.

[3] M.M. Paulides, "Development of a clinical head and neck hyperthermia applicator", PhD dissertation, October 18, 2007, Erasmus University Rotterdam.

[4] Alberti G., Ciofaniello L., Galiero G., Persico R., Sacchettino M., Signore G.M., Vetrella S., ‘Experimental results from a stepped frequency GPR’, Annals of Geophysics 46 (4): p.707-717, Augustus 2003.

[5] Soldovieri F., Leone G., Liseno A., Tartaglione F., Pierri R., ‘Linear tomographic inversion of stepped-frequency GPR data: experimental results on two test-sites’, AEU-International Journal of Electronics and Communications, 59 (6): p.329-336, 2005.

[6] Korkmaz E., van Genderen P., ‘Calibration procedures for antenna footprint measurement of stepped frequency CW radar’’, Proceedings of the Tenth International Conference on Ground Penetrating Radar, Volume 1, p.129 – 132, 21-24 June 2004, Delft, The Netherlands.

[7] Korkmaz E., van Genderen P., ‘Antenna footprint measurements of stepped frequency CW radar on the air/ground interface’, IEE Antenna Measurements and SAR, p.87 – 91, 25-26 May 2004, Loughbrough, UK.

[8] S. Xiao, B. Z. Wang, and X. S. Yang, “A Novel Frequency Reconfigurable Patch Antenna,” Microwave Opt. and Technol.Lett., 36, Feb. 2003, pp. 295-297.

[9] Broadband Microstrip Antennas, 1st edition, Girish Kumar and K.P.Ray, Artech House Publisher, Norwood, 2003.

[10] K. Chung, Y. Nam, T. Yun, and J. Choi, “Reconfigurable Microstrip Patch Antenna with Switchable Polarization”, ETRI Journal, Volume 28, Number 3, June 2006

[11] D. M. Pozar and D. H. Schaubert, “Scan Blindness in Infinite Phased Arrays of Printed Dipoles,” IEEE Trans. Antennas Propagat., Vol. AP-32, No. 6, pp. 602–610, June 1984.

[12] F. Zavosh and J. T. Aberle, “Infinite Phased Arrays of Cavity-Backed Patches,” Vol. AP-42,No. 3, pp. 390–398, March 1994.

[13] D. H. Schaubert, D. M. Pozar, and A. Adrian, “Effect of Microstrip Antenna Substrate Thickness and Permittivity: Comparison of Theories and Experiment,” IEEE Trans. Antennas Propagat., Vol. AP-37, No. 6, pp. 677–682, June 1989.

[14] L. C. Shen, S. A. Long, M. R. Allerding, and M. D. Walton, “Resonant Frequency of a Circular Disc, Printed-Circuit Antenna,” IEEE Trans. Antennas Propagat., Vol. AP-25, No. 4, pp. 595–596, July 1977.

[15] F. Zavosh and J. T. Aberle, “Infinite Phased Arrays of Cavity-Backed Patches,” Vol. AP-42, No. 3, pp. 390–398, March 1994.

[16] Paul E. Mayes, “Frequency-Independent Antennas and Broad-Band Derivatives Thereof”, Proceedings of the IEEE, Volume: 80 , Issue: 1, Digital Object Identifier: 10.1109/5.119570, Publication Year: 1992, Page(s): 103 – 112

[17] Stephen E. Lipsky "Microwave Passive Direction Finding " SciTech Publishing, 2004 ISBN 1891121235 page 40

[18] J. Q. Howell, Microstrip antenna, IEEE Trans. Antennas Propag., Vol. 23, pp. 90–93, January 1975.

[19] T. C. Edwards, “Foundations for Microstrip Circuit Design,” John Wiley & Sons, USA, 1981.

[20] Kaiser, J. A., \The Archimedean two-wire spiral antenna," IRE Trans. Antennas and Propagation, Vol. 8, No. 3, 312{323, 1986.

[21] I. J. Bahl and P. Bhartia, Microstrip Antennas, Artech House, Dedham, MA, 1980.

[22] K. R. Carver and J. W. Mink, “Microstrip Antenna Technology,” IEEE Trans. Antennas Propagat., Vol. AP-29, No. 1, pp. 2–24, January 1981.

[23] W. F. Richards, “Microstrip Antennas,” Chapter 10 in Antenna Handbook: Theory, Applications and Design (Y. T. Lo and S. W. Lee, eds.), Van Nostrand Reinhold Co., New York,1988.

[24] Stutzman, W.L. and Thiele, G.A., Antenna Theory and Design, John Wiley & Sons, Inc, 1998.

[25] D. M. Pozar, “Considerations for Millimeter-Wave Printed Antennas,” IEEE Trans. Antennas Propagat., Vol. AP-31, No. 5, pp. 740–747, September 1983.

[26] J. R. James and P. S. Hall, Handbook of Microstrip Antennas, Peter Peregrinus Ltd., London, 1989.

[27] Kuboyama, H., et al. “Post Loaded Microstrip Antenna for Pocket Size Equipment at UHF,” proc. Isap, 1985, pp. 433-436.

[28] Balanis, C.A., Antenna Theory: Analysis and Design, John Wiley & Sons, Inc, 1997.

[29] E. H. Van Lil and A. R. Van de Capelle, “Transmission-Line Model for Mutual Coupling Between Microstrip Antennas,” IEEE Trans. Antennas Propagat., Vol. AP-32, No. 8, pp. 816–821, August 1984.

[30] Balanis, C.A., Antenna Theory: Analysis and Design, John Wiley & Sons, Inc, 2005.

[31] Huang, Yi and Boyle K., Antennas from Theory to Practice, John Wiley & Sons. Inc, 2008

APPENDIX A

S-PARAMETERS OF RSMPA 10X10.5 CM.

First Case

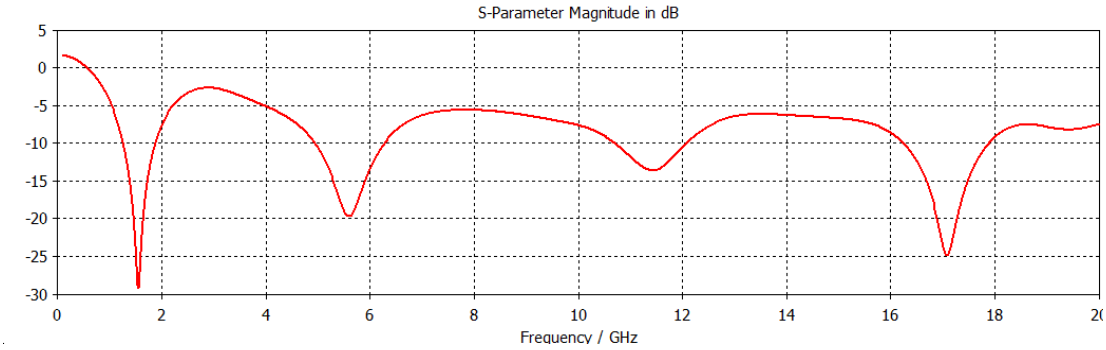

Second Case

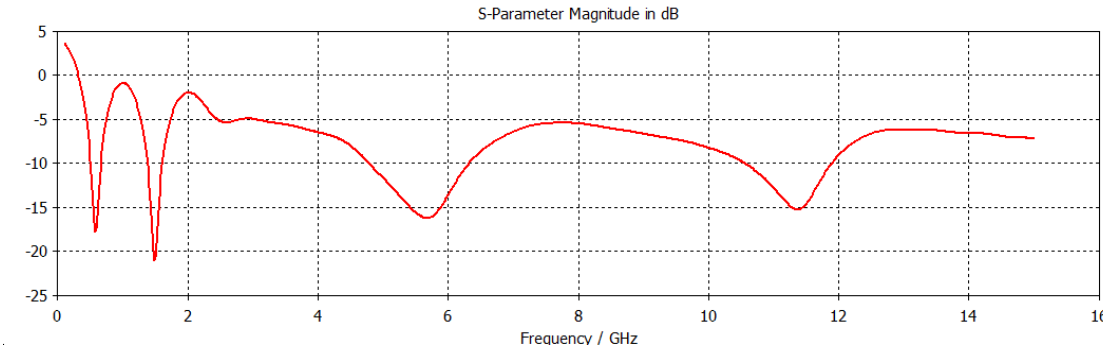

Third Case

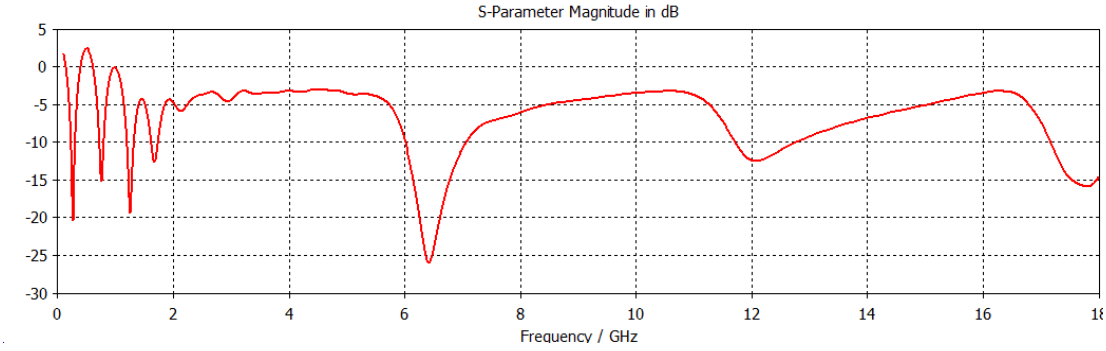

S-PARAMETERS OF RSMPA 3.5X3.7 CM.

First Case

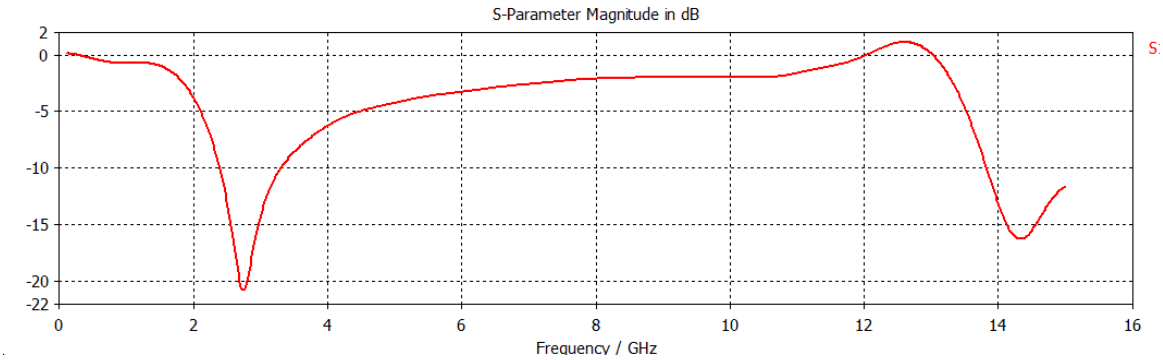

Second Case

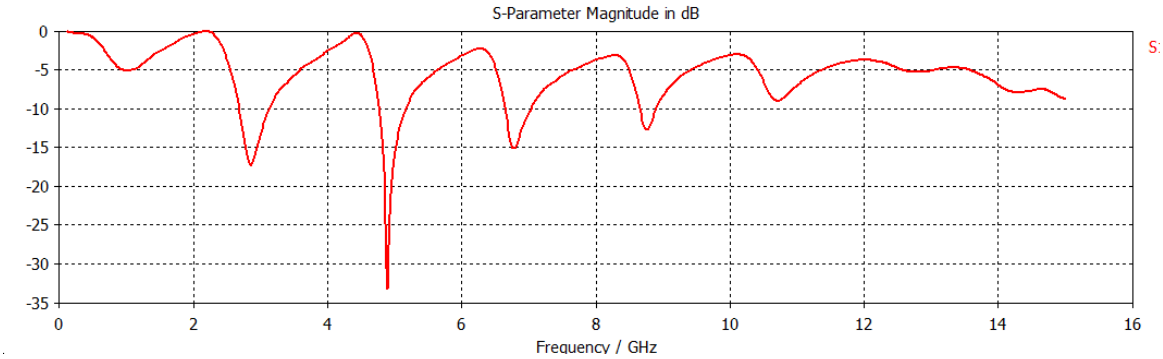

Third Case

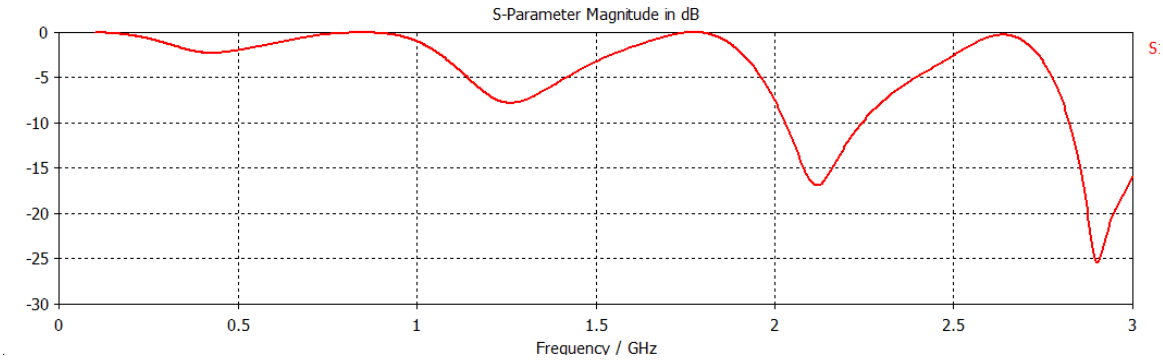

S-PARAMETERS OF CSMPA 2.8X2.8 CM.

First Case

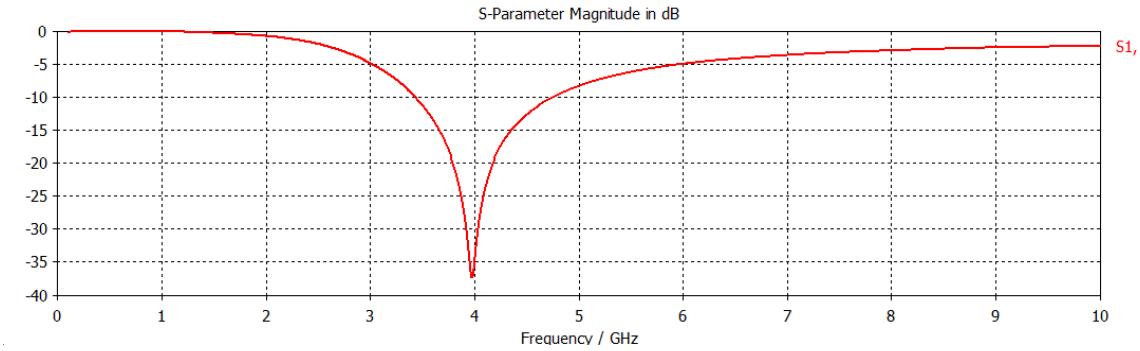

Second Case

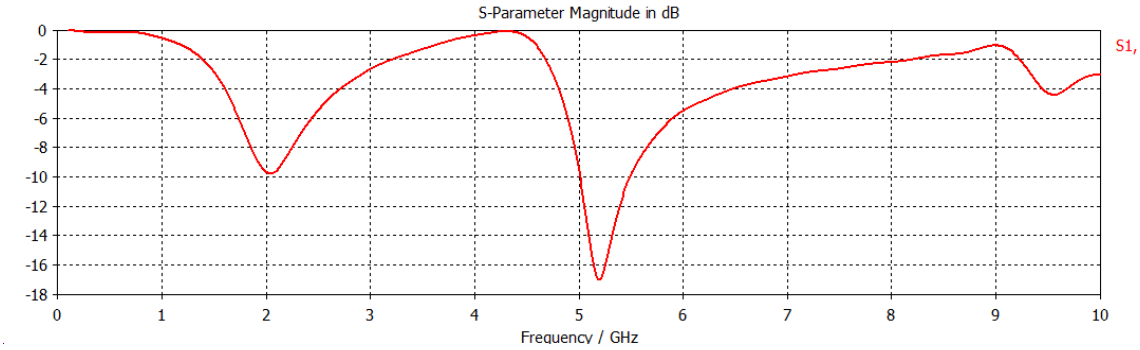

Third Case

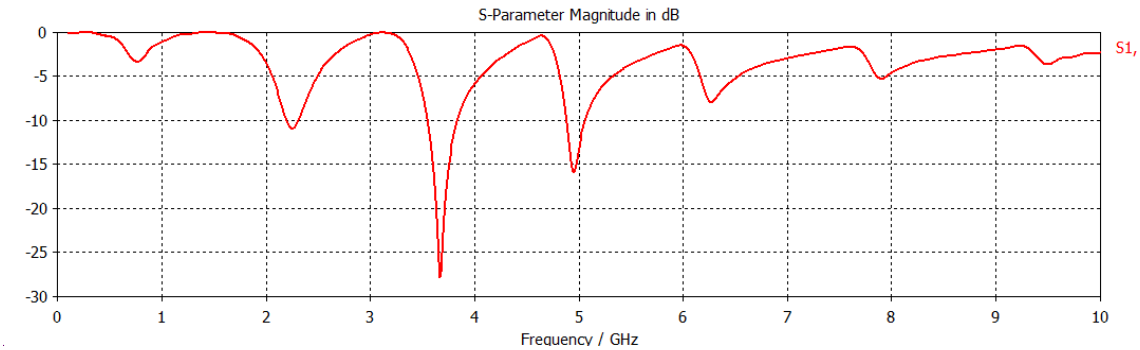

Filename:	Thesis_Ashraf
Directory:	C:\Users\pc\Documents
Template:	C:\Users\pc\AppData\Roaming\Microsoft\Templates\Normal.dotm
Title:	
Subject:	
Author:	pc
Keywords:	
Comments:	
Creation Date:	1/24/2011 9:15:00 PM
Change Number:	444
Last Saved On:	7/1/2011 11:23:00 PM
Last Saved By:	pc
Total Editing Time:	16,621 Minutes
Last Printed On:	7/2/2011 11:02:00 AM
As of Last Complete Printing	
Number of Pages:	84
Number of Words:	14,282 (approx.)
Number of Characters:	81,408 (approx.)